Synthesis and characterization of oligodeoxyribonucleotides modified with 2′-thio-2′-deoxy-2′-*S*-(pyren-1-yl)methyluridine

Brooke A. Anderson and Patrick J. Hrdlicka

Department of Chemistry, University of Idaho, Moscow, ID 83844

SUPPORTING INFORMATION

General experimental section. Reagents and solvents were commercially available, of analytical grade and used without further purification. Petroleum ether of the distillation range 60-80 °C was used. Solvents were dried over activated molecular sieves: *N*,*N*-dimethylformamide (3Å); pyridine, CH_2Cl_2, 1,2-dichloroethane, triethylamine, and *N,N*-diisopropylethylamine (4Å). Water content of anhydrous solvents was verified on Karl-Fisher apparatus. Reactions were monitored by TLC using silica gel coated plates with a fluorescence indicator (SiO_2-60, F-254) which were visualized a) under UV light and/or b) by dipping in 5% conc. H_2SO_4 in absolute ethanol (v/v) followed by heating. Silica gel column chromatography was performed with Silica gel 60 (particle size 0.040–0.063 mm) using moderate pressure (pressure ball). Evaporation of solvents was carried out under reduced pressure at temperatures below 45 °C. After column chromatography, appropriate fractions were pooled, evaporated and dried at high vacuum for at least 12 h to give the obtained products in high purity (>95%) as ascertained by 1D NMR techniques. Exchangeable (ex) protons were detected by disappearance of signals upon D_2O addition. Assignments of NMR spectra are based on 2D spectra (COSY, HSQC) and DEPT spectra. Quaternary carbons are not assigned in ^{13}C NMR but verified from HSQC and DEPT spectra (absence of signals). MALDI-HRMS spectra of compounds were recorded on a mass spectrometer using 2,5-dihydroxybenzoic acid as a matrix and polyethylene glycol (PEG 600) as an internal calibration standard.

Synthetic protocols.

2′-Deoxy-2′-*S*-(pyren-1-yl)methyl-2′-thiouridine (2). To a flame-dried round-bottomed flask flushed with argon, was added nucleoside **1**[S1] (250 mg, 0.96 mmol), 1-pyrenylmethyl chloride (360 mg, 1.44 mmol), anhydrous DMF (6 mL), and anhydrous Et_3N (200 µL, 1.44 mmol). The reaction mixture was stirred at room temperature under an argon atmosphere for 17h whereupon it was

diluted with EtOAc (100 mL) and washed with brine (2 x 30 mL), saturated aqueous $NaHCO_3$ (30 mL) and H_2O (30 mL). The organic layer was dried (Na_2SO_4) and evaporated to dryness. The resulting residue was purified by silica gel column chromatography (0-7 % MeOH in CH_2Cl_2, v/v) to afford nucleoside **2** as a pale yellow solid (290 mg, 64%). R_f = 0.3 (10 % MeOH in CH_2Cl_2); MALDI-HRMS 497.1148 ($[M+Na]^+$, $C_{26}H_{22}N_2O_5S{\cdot}Na^+$, Calcd. 497.1142); ^{1}H NMR (500 MHz, DMSO-d_6) δ 11.40 (br s, 1H, ex, NH), 8.37-8.40 (d, 1H, J = 9.3 Hz, Py), 8.28-8.31 (2d, 2H, J = 7.8 Hz, 7.5 Hz, Py), 8.21-8.24 (d, 1H, J = 9.3 Hz, Py), 8.18-8.21 (d, 1H, J = 7.8 Hz, Py), 8.15-8.18 (d, 1H, J = 9.1 Hz, Py), 8.12-8.15 (d, 1H, J = 9.1 Hz, Py), 8.06-8.10 (t, 1H, J = 7.5 Hz, Py), 7.94-7.97 (d, 1H, J = 7.8 Hz, Py), 7.79 (d, 1H, J = 8.3 Hz, H6), 6.21 (d, 1H, J = 8.5 Hz, H1′), 5.72 (d, 1H, ex, J = 5.5 Hz, 3′-OH), 5.53 (d, 1H, J = 8.5 Hz, H5), 5.10 (t, 1H, ex, J = 5.2 Hz, 5′-OH), 4.52-4.55 (d, 1H, J = 12.0 Hz, CH_2), 4.48-4.51 (d, 1H, J = 12.2 Hz, CH_2), 4.25-4.29 (m, 1H, H3′), 3.91-3.94 (m, 1H, H4′), 3.56-3.66 (m, 3H, H2′, H5′); ^{13}C NMR (75.5 MHz, DMSO-d_6) δ 162.7, 150.8, 140.1 (C6), 131.6, 130.7, 130.3, 130.2, 128.4, 127.9 (Py), 127.4 (Py), 127.3 (Py), 127.1 (Py), 126.3 (Py), 125.25 (Py), 125.17 (Py), 124.7 (Py), 124.2, 123.8, 123.5 (Py), 102.3 (C5), 87.6 (C1′), 86.6 (C4′), 71.9 (C3′), 61.3 (C5′), 52.5 (C2′), 32.6 (CH_2Py).

2′-Deoxy-5′-*O*-(4,4′-dimethoxytrityl)-2′-*S*-(pyren-1-yl)methyl-2′-thiouridine (3). Nucleoside **2** (200 mg, 0.42 mmol) was coevaporated with anhydrous 1,2-dichloroethane (2 × 5 mL) and re-dissolved in anhydrous pyridine (5 mL). To this was added 4,4′-dimethoxytritylchloride (DMTrCl, 186 mg, 0.55 mmol) and a catalytic amount of 4-dimethylaminopyridine (DMAP, ~5 crystals). The reaction mixture was stirred at room temperature under an argon atmosphere for 19 h, when it was diluted with CH_2Cl_2 (40 mL) and washed with saturated aqueous $NaHCO_3$ (30 mL). The aqueous layer was back-extracted with CH_2Cl_2 (3 × 15 mL) and the combined organic layers were

dried (Na_2SO_4), evaporated to dryness and co-evaporated with absolute EtOH and toluene (2:1 v/v, 3 × 20 mL). The resulting residue was purified by silica gel column chromatography (0-6% MeOH in CH_2Cl_2, v/v) to yield nucleoside **3** as a tan-colored foam (236 mg, 72%). R_f = 0.7 (10% MeOH in CH_2Cl_2, v/v); MALDI-HRMS *m/z* 799.2474 ($[M+Na]^+$, $C_{47}H_{40}N_2O_7S{\cdot}Na^+$, Calcd. 799.2448); ^{1}H NMR (500 MHz, DMSO-d_6) δ 11.48 (d, 1H, ex, J = 2.0 Hz, NH), 8.38-8.41 (d, 1H, J = 9.0 Hz, Py), 8.28-8.31 (d, 2H, J = 7.5 Hz, Py), 8.21-8.24 (d, 1H, J = 9.0 Hz, Py), 8.11-8.18 (m, 3H, Py), 8.06-8.10 (t, 1H, J = 7.5 Hz, Py), 7.95-7.98 (d, 1H, J = 8.0 Hz, Py), 7.64 (d, 1H, J = 8.0 Hz, H6), 7.35-7.38 (m, 2H, DMTr), 7.29-7.33 (m, 2H, DMTr), 7.21-7.26 (m, 5H, DMTr), 6.85-6.88 (m, 4H, DMTr), 6.21 (d, 1H, J = 7.5 Hz, H1′), 5.77 (d, 1H, ex, J = 5.5 Hz, 3′-OH), 5.42 (dd, 1H, J = 8.0 Hz, 2.0 Hz, H5), 4.57-4.60 (d, 1H, J = 12.0 Hz, CH_2), 4.50-4.54 (d, 1H, J = 12.0 Hz, CH_2), 4.21-4.25 (m, 1H, H3′), 3.98-4.02 (m, 1H, H4′), 3.66-3.75 (m, 7H, H2′, CH_3O), 3.26-3.31 (m, 1H, H5′), 3.20-3.24 (m, 1H, H5′); ^{13}C NMR (125 MHz, DMSO-d_6) δ 162.7, 158.1, 150.6, 144.6, 140.1 (C6), 135.3, 135.2, 131.5, 130.7, 130.3, 130.2, 129.70 (DMTr), 129.68 (DMTr), 128.4, 127.84 (DMTr), 127.76 (Py), 127.6 (DMTr), 127.4 (Py), 127.3 (Py), 127.2 (Py), 126.7 (DMTr), 126.3 (Py), 125.3 (Py), 125.2 (Py), 124.7 (Py), 124.2, 123.8, 123.5 (Py), 113.20 (DMTr), 113.19 (DMTr), 102.2 (C5), 88.1 (C1′), 85.9, 84.5 (C4′), 71.2 (C3′), 63.5 (C5′), 55.0 (CH_3O), 52.3 (C2′), 32.6 (CH_2Py).

2′-Deoxy-3′-*O*-(*N*,*N*-diisopropylamino-2-cyanoethoxyphosphinyl)-5′-*O*-(4,4′-dimethoxytrityl)-2′-*S*-(pyren-1-yl)methyl-2′-thiouridine (4). Nucleoside **3** (160 mg, 0.21 mmol) was coevaporated with anhydrous 1,2-dichloroethane (2 × 3 mL) and re-dissolved in anhydrous CH_2Cl_2 (3 mL). To this was added anhydrous *N*,*N*-diisopropylethylamine (DIPEA, 145 μL, 0.82 mmol) followed by dropwise addition of 2-cyanoethyl-*N*,*N*-

diisopropylchlorophosphoramidite (CEP-Cl, 92 μL, 0.41 mmol). The reaction mixture was stirred under an argon atmosphere at room temperature for 2 h when absolute EtOH (0.5 mL) was added. Solvents were evaporated off and the resulting residue was purified by silica gel column chromatography (0-60% EtOAc in petroleum ether, v/v) followed by precipitation from CH_2Cl_2 and petroleum ether to afford nucleoside **4** as a tan-colored foam (146 mg, 73%). R_f = 0.6 (3% MeOH in CH_2Cl_2, v/v); MALDI-HRMS *m/z* 999.3487 ($[M+Na]^+$, $C_{56}H_{57}N_3O_8S{\cdot}Na^+$, Calcd. 999.3527); ^{31}P NMR (121 MHz, $CDCl_3$) δ 150.9, 149.9.

Protocol – pseudorotational analysis of nucleosides. A Matlab-based pseudorotational analysis program[S2] was used to determine P and ϕ_m for the furanose ring of nucleoside **3** from $^3J_{HH}$ scalar coupling constants of the endocyclic sugar protons. Appropriate electronegativity (ε_{en}) values for the β-D-ribose ring and the C_2'-substituents were selected from the electronegativity editor interface using DMSO solvent values: OR (ε_{en} = 1.400), NR_2 (ε_{en} = 1.200) and SR (ε_{en} = 0.785). Coupling constants for $^3J_{H1'H2'}$, $^3J_{H2'H3'}$, and $^3J_{H3'H4'}$ were obtained from ^1H NMR (500 MHz, DMSO-d_6, 25 °C) data analysis. Two prototypical North and South conformations (P_A = 18°, P_B = 153.6°, ϕ_m = 38°, proportion of conformer A = 30-50 %) were chosen as starting structures for fitting of the modified Karplus-Diez-Donders equations to the experimental $^3J_{HH}$ coupling constants.[S2-S4] The process was repeated in an iterative manner using the main *North* and *South* type conformations from the previous run as seed structures, until no further significant conformational changes were observed (typically 3 runs). The key features of the optimized conformers and their relative proportions are reported in Table S1.

Protocol - synthesis and purification of ONs. Modified ONs were synthesized on a 0.2 μmol scale using a DNA synthesizer and succinyl linked LCAA-CPG (long chain alkyl amine controlled pore glass) columns with a pore size of 500Å. Standard protocols for incorporation of DNA monomers were used. Extended hand-coupling conditions (15 min) were used for incorporation of monomer **S** using 4,5-dicyanoimidazole as an activator with >95% coupling yield. Extended oxidation (45s) was used. Cleavage from solid support and removal of protecting groups was accomplished using 32% aqueous ammonia (55 °C, 12 h). ONs were purified in the DMTr-on mode via ion-pair reverse phase HPLC (C18 column) using a 0.05 M triethylammonium acetate - water/acetonitrile gradient. This was followed by detritylation (80% aqueous AcOH) and precipitation ($NaOAc/NaClO_4$/acetone, -18 °C for 12-16 h). The identity of synthesized ONs was established through MALDI-MS analysis recorded in positive ion mode on a quadrupole time-of-flight tandem mass spectrometer equipped with a MALDI source using anthranilic acid, 3-hydroxypicolinic acid (3-HPA) as a matrix (Table S2). Purity was verified by ion-pair reverse phase HPLC running in analytical mode (>90%).

Protocol - thermal denaturation studies. ON concentrations were estimated using the following extinction coefficients for DNA (OD/μmol): G (12.01), A (15.20), T (8.40), C (7.05); RNA (OD/μmol): G (13.70), A (15.40), U (10.00), C (9.00); and pyrene (22.4)[S5]. Strands were thoroughly mixed and denatured by heating to 70 °C, followed by cooling to the starting temperature of the experiment. Quartz optical cells with a path length of 1.0 cm were used. Thermal denaturation temperatures of duplexes (1.0 μM final concentration of each strand) were measured using a UV/vis spectrophotometer equipped with a 12-cell Peltier temperature controller and determined as the maximum of the first derivative of the thermal denaturation curve (A_{260} vs.

T) recorded in medium salt phosphate buffer (T_m buffer: 100 mM NaCl, 0.1 mM EDTA; pH 7.0 adjusted with 10 mM Na_2HPO_4 and 5 mM Na_2HPO_4). The temperature of the denaturation experiments ranged from at least 15 °C below T_m (although not below 3 °C) to 20 °C above T_m. A temperature ramp of 0.5 °C/min was used in all experiments. Reported T_m's are averages of two experiments within ± 1.0 °C.

Protocol - determination of thermodynamic parameters. Thermodynamic parameters for duplex formation were determined through baseline fitting of denaturation curves using software provided with the UV/Vis spectrometer. Bimolecular reactions, two-state melting behavior, and a heat capacity change of $\Delta C_p = 0$ upon hybridization were assumed.[S6] A minimum of two experimental denaturation curves were each analyzed at least three times to minimize errors arising from baseline choice. Averages and standard deviations are listed.

Protocol - absorption spectra. UV-Vis absorption spectra (range 200-600 nm) were recorded at 10 °C using the same samples and instrumentation as used in the thermal denaturation experiments.

Protocol - steady-state fluorescence emission spectra. Steady-state fluorescence emission spectra of **S**-modified ONs modified and the corresponding duplexes with cDNA/cRNA, were recorded in non-deoxygenated thermal denaturation buffer (each strand at 1.0 μM concentration) and obtained as an average of five scans using an excitation wavelength of $\lambda_{ex} = 350$ nm. Excitation and emission slits of 5.0 nm and 2.5 nm, respectively were used along with a scan speed of 600 nm/min. Experiments were determined at 10 °C with N_2 flow to ascertain maximal hybridization of probes to DNA/RNA targets and minimize condensation, respectively.

Protocol - electrophoretic mobility shift assay. This assay was performed essentially as previously described.[S7] Unmodified DNA hairpin **DH1** was obtained from commercial sources and used without further purification. The DNA hairpin was 3′-DIG-labeled using the 2nd generation DIG Gel Shift Kit (Roche Applied Bioscience) as recommended by the manufacturer. The DIG-labeled ON obtained in this manner was diluted and used without further purification in the recognition experiments. Pre-annealed probe (85 °C for 10 min, cooled to room temperature over 15 min) and DIG-labeled DNA hairpins (34.4 nM) were mixed and incubated in HEPES buffer (50 mM HEPES, 100 mM NaCl, 5 mM $MgCl_2$, 10% sucrose, 1.44 mM spermine tetrahydrochloride, pH 7.2) for the specified time at ambient temperature (~21±3 °C). The reaction mixtures were then diluted with 6x DNA loading dye (Fermentas) and loaded onto a 16% non-denaturing polyacrylamide gel. Electrophoresis was performed using a constant voltage of 70 V for 2.5 h at ~4 °C using 0.5x TBE as a running buffer (45 mM Tris, 45 mM boric acid, 1 mM EDTA). Gels were blotted onto positively charged nylon membranes (Roche Applied Bioscience) using constant voltage with external cooling (100V, ~4 °C). The membranes were exposed to anti-digoxigenin-AP F_{ab} fragments as recommended by the manufacturer of the DIG Gel Shift Kit, transferred to a hybridization jacket, and incubated with the substrate (CSPD) in detection buffer for 10 min at 37 °C. The chemiluminescence of the formed product was captured on X-ray film, which was developed using an X-Omatic 1000A X-ray film developer (Kodak). The resulting bands were quantified using Image J software. Invasion efficiency was determined as the intensity ratio between the recognition complex band and the total lane. An average of three independent experiments is reported.

Definition of zipper nomenclature. The following nomenclature describes the relative arrangement between two monomers positioned on opposing strands in a duplex. The number *n* describes the distance measured in number of base pairs and has a positive value if a monomer is shifted toward the 5′-side of its own strand relative to a second reference monomer on the other strand. Conversely, *n* has a negative value if a monomer is shifted toward the 3′-side of its own strand relative to a second reference monomer on the other strand.

Table S1. $^3J_{HH}$ scalar coupling constants, pseudorotation phase angles (P) and puckering amplitudes (ϕ_m) for nucleoside **3** (monomer **S**) and the corresponding nucleosides for monomer **O** and **N**.

Monomer	**S**	**O**	**N**
$J_{1'-2'}$	7.5	4.1[a]	8.3[a]
$J_{2'-3'}$	6.0	4.9[a]	5.7[a]
$J_{3'-4'}$	3.9	5.8[a]	2.3[a]
Conformation I			
P	56.5	11.0	121.6[‡]
ϕ_m	26.9	38.4	27.4
Conformation II			
P	143.0	130.3	145.1[‡]
ϕ_m	37.5	33.4	37.8
% Conformation II	61	49	61

[‡]The Matlab script was unable to fit the data for this nucleoside to a *North* type conformations, despite different input conditions. Invariably, two *South* type conformations were predicted.

[a]Data from reference S8.

Table S2. MALDI-MS of ONs modified with monomer **S**.[a]

ONs	Sequence	Calc. *m/z* $[M+H]^+$	Found *m/z* $[M+H]^+$
S1	5′-G**S**G ATA TGC	2985.5	2985.8
S2	5′-GTG A**S**A TGC	2985.5	2985.8
S3	5′-GTG ATA **S**GC	2985.5	2984.7
S4	3′-CAC **S**AT ACG	2914.5	2914.8
S5	3′-CAC TA**S** ACG	2914.5	2914.8
S6	3′-CAC **S**A**S** ACG	3146.6	3146.9

[a] For structure of monomer **S**, see Figure 1 in the main manuscript.

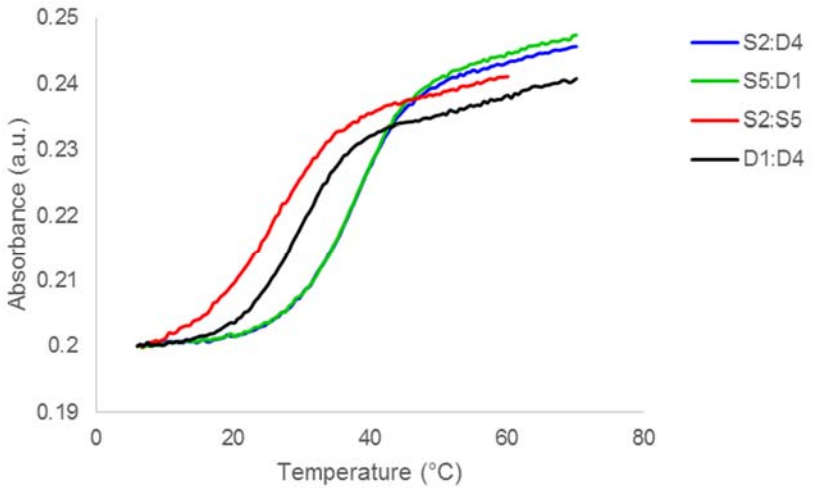

Figure S1. Representative thermal denaturation curves of **S**-modified duplexes and reference duplex **D1**:**D4**. For experimental conditions, see Table 1.

Additional discussion regarding DNA-selectivity. The DNA selectivity, defined as $\Delta\Delta T_m$ (DNA-RNA) = ΔT_m (vs cDNA) - ΔT_m (vs cRNA) > 0 °C, of **S**-modified ONs is very similar to the DNA selectivity observed for **O**- and **N**-modified ONs ($\Delta\Delta T_m$ from +9.0 to +16.5 °C, Table S3), indicating that the pyrene moiety of **S**-modified ONs likely has a similar binding mode as in **O**- and **N**-modified ONs.

Table S3. DNA selectivity of **B1-B6**.[a]

			$\Delta\Delta T_m$/mod (DNA-RNA) [°C]		
ON	**Duplex**	**B =**	**S**	**O**[b]	**N**[b]
B1	5′-G**B**G ATA TGC		+9.0	+7.0	+9.5
B2	5′-GTG A**B**A TGC		+10.0	+8.5	+12.5
B3	5′-GTG ATA **B**GC		+9.5	+8.0	+8.5
B4	3′-CAC **B**AT ACG		+10.0	+8.0	+8.5
B5	3′-CAC TA**B** ACG		+10.0	+9.0	+12.5
B6	3′-CAC **B**A**B** ACG		+16.5	+15.0	+18.5

[a] DNA selectivity defined as $\Delta\Delta T_m$ (DNA-RNA) = ΔT_m (vs cDNA) - ΔT_m (vs cRNA).
[b] From reference S8.

Additional discussion of DNA/RNA binding specificity. Reference strand **D1** displays the expected specificity profile against mismatched RNA targets, i.e., mismatched duplexes have lower T_m's than matched duplexes, with T:rG being the least efficiently discriminated mismatched base pair (Table S4). Singly modified **S2** and benchmark ONs **O2** and **N2** have comparable binding specificity profiles except for significantly decreased discrimination of T:U pairs.

The binding specificities of ONs with two next-nearest neighbor modifications (**B6**-series) were determined using DNA targets with a mismatched nucleotide opposite of the central 2'-deoxyriboadenosine (Table S5). We have previously shown that **O6** and **N6** display unexpectedly good binding specificity compared to the poor binding specificities of **O2** and **N2** (Table 2). Interestingly, **S6** discriminates the mismatched DNA targets less efficiently than **O6** and **N6**, which suggests that the sulfur of monomer **S** interferes with the binding mode leading to improved binding specificity.

Table S4. Discrimination of mismatched RNA targets by **B2**-series and reference strands.[a]

			RNA: 3′-CAC U**B**U ACG			
			T_m [°C]	ΔT_m [°C]		
ON	**Sequence**	**B** =	**A**	C	G	U
D1	5′ – GTG ATA TGC		**27.5**	<-17.5	-4.5	<-17.5
S2	5′ – GTG A**S**A TGC		**25.5**	<-15.5	-5.5	-8.5
O2[b]	5′ – GTG A**O**A TGC		**31.5**	-17.5	-3.5	-9.5
N2[b]	5′ – GTG A**N**A TGC		**30.5**	-16.5	-0.5	-13.0

[a] For conditions of thermal denaturation experiments, see Table 1. T_m's of fully matched duplexes are shown in bold. ΔT_m = change in T_m relative to fully matched DNA:RNA duplex.

[b] From reference S8.

Table S5. Discrimination of mismatched DNA targets by **S6**/**O6**/**N6** and reference strands.[a]

			DNA: 5′-GTG A**B**A TGC			
			T_m [°C]	ΔT_m [°C]		
ON	**Sequence**	**B**=	**T**	A	C	G
D4	3′-CAC TAT ACG		**29.5**	-17.0	-15.5	-9.0
S6	3′-CAC **S**A**S** ACG		**37.5**	-12.5	-12.0	-12.0
O2[b]	3′-CAC **O**A**O** ACG		**43.5**	-24.0	-17.0	-14.0
N2[b]	3′-CAC **N**A**N** ACG		**43.5**	-21.5	-10.5	-13.5

[a]For conditions of thermal denaturation experiments, see Table 1. T_m's of fully matched duplexes are shown in bold. ΔT_m = change in T_m relative to fully matched duplex

[b]From reference S8.

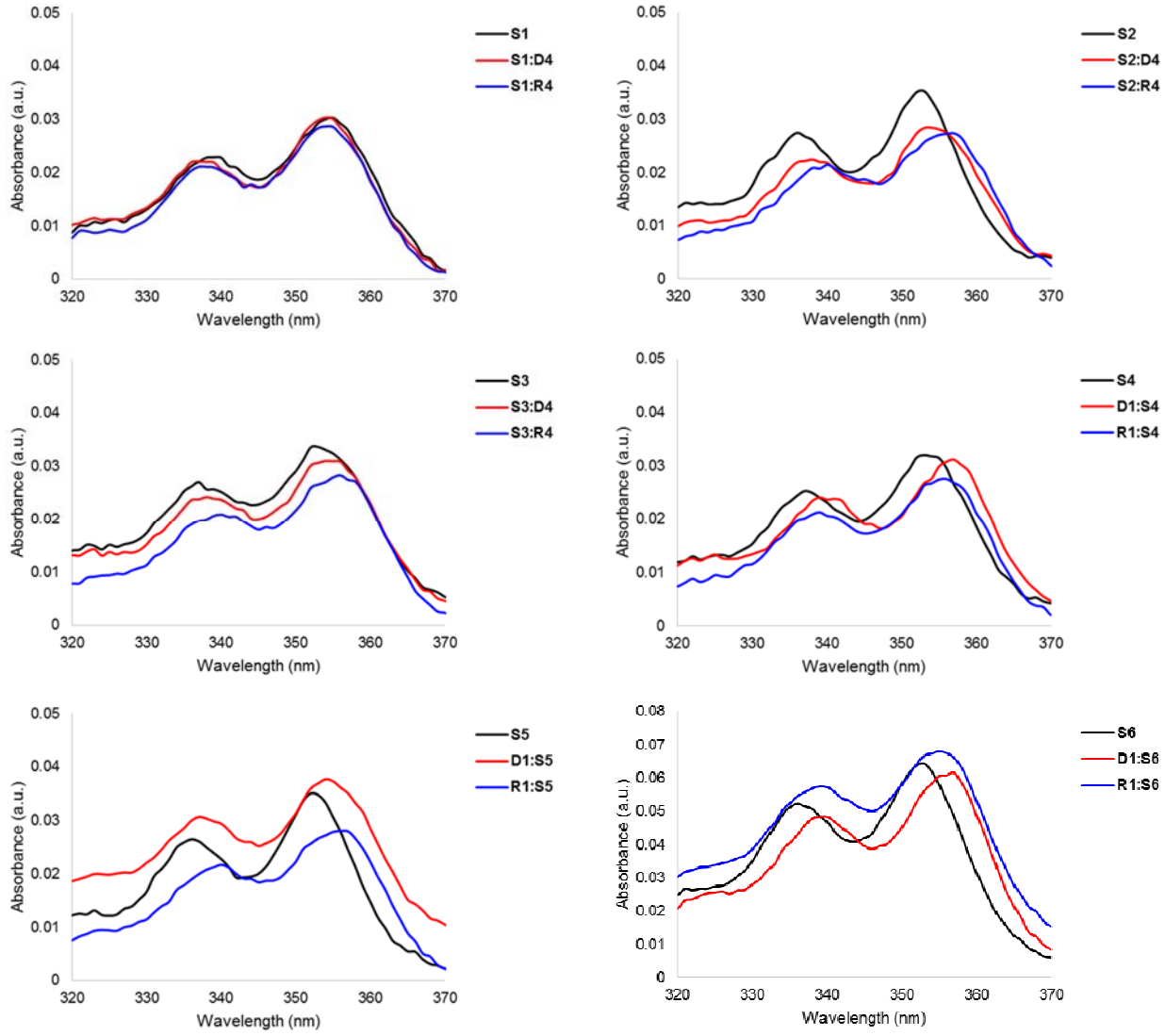

Figure S2. Absorption spectra of single-stranded **S1**-**S6** and the corresponding duplexes with cDNA/cRNA targets. Spectra were recorded at T = 10 °C using each strand at 1.0 μM concentration in T_m buffer. Note that a different Y-axis scale is used for **S6**.

Discrimination of mismatched DNA targets via fluorescence. Neither singly or doubly **S**-modified ONs allow for discrimination of DNA targets with centrally mismatched nucleotides via fluorescence (Figure S3). Thus, **S**-modified ONs have limited potential as probes for fluorescent discrimination of single nucleotide polymorphisms (SNPs).

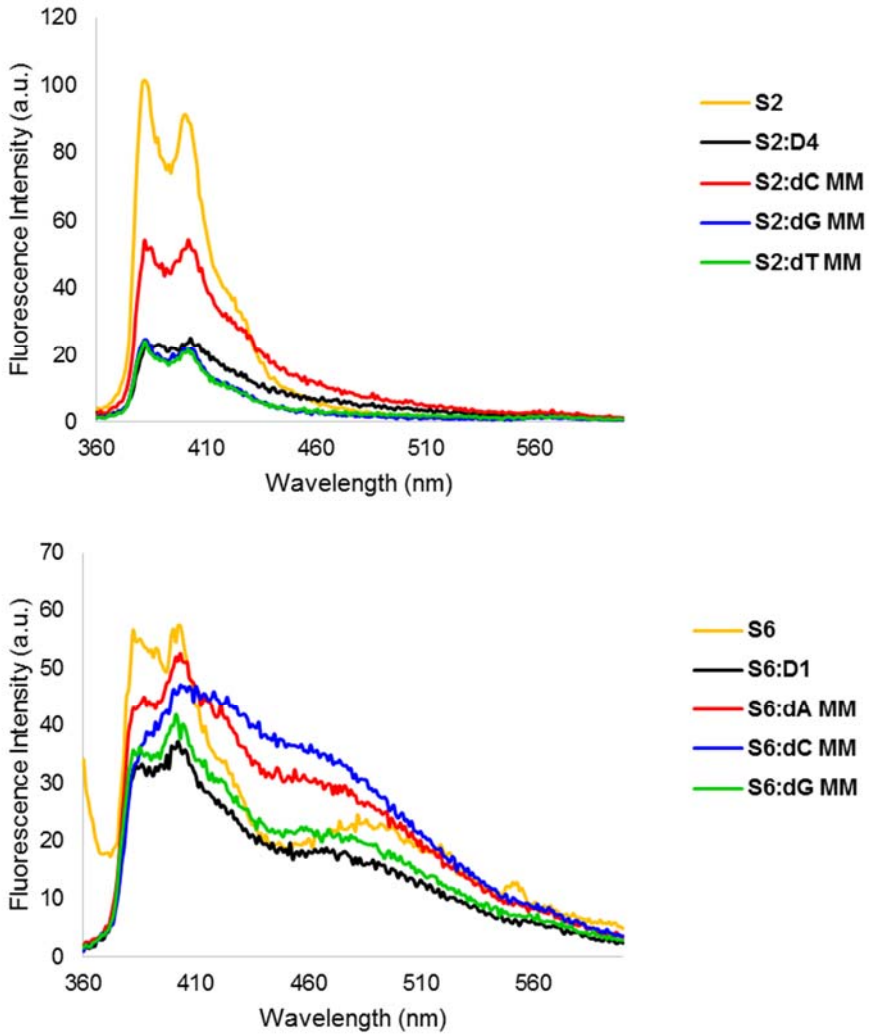

Figure S3. Steady-state fluorescence emission spectra of **S2** and **S6** against matched and centrally mismatched DNA targets (mismatched nucleotide specified). Spectra were recorded at $T = 10$ °C using $\lambda_{ex} = 350$ nm and each strand at 1.0 μM concentration in T_m buffer.

Table S6. Change in enthalpy upon duplex formation (ΔH) and reaction enthalpy for recognition of isosequential dsDNA target **D1**:**D4** (ΔH_{rec}).[a]

ON	ZP	Sequence	ΔH [$\Delta\Delta H$] (kJ/mol) upper ON vs cDNA	lower ON vs cDNA	probe duplex	ΔH_{rec} (kJ/mol)
S1 **S5**	**+4**	5′-G**S**G ATA TGC 3′-CAC TA**S** ACG	-308±3 [-22]	-331±9 [-45]	-356±8 [-70]	+3
S1 **S4**	**+2**	5′-G**S**G ATA TGC 3′-CAC **S**AT ACG	-308±3 [-22]	-314±4 [-28]	-260±6 [+26]	-76
S2 **S5**	**+1**	5′-GTG A**S**A TGC 3′-CAC TA**S** ACG	**-320±6 [-34]**	**-331±9 [-45]**	**-275±10 [+11]**	**-90**
S2 **S4**	**-1**	5′-GTG A**S**A TGC 3′-CAC **S**AT ACG	-320±6 [-34]	-314±4 [-28]	-316±4 [-30]	-32

[a] $\Delta\Delta H$ is measured relative to ΔH for **D1**:**D4** = -286 kJ/mol. ΔH_{rec} = ΔH (upper ON vs cDNA) + ΔH (lower ON vs cDNA) - ΔH (probe duplex) - ΔH (**D1**:**D4**). "ZP" and "±" denotes zipper and standard deviation, respectively.

Table S7. Change in entropy at 293K upon duplex formation ($-T^{293}\Delta S$) and reaction entropy for recognition of isosequential dsDNA target **D1**:**D4** ($-T^{293}\Delta S_{rec}$).[a]

Duplex	ZP	Sequence	$-T^{293}\Delta S$ [$\Delta(T^{293}\Delta S)$] (kJ/mol) upper ON vs cDNA	lower ON vs cDNA	probe duplex	$-T^{293}\Delta S_{rec}$ (kJ/mol)
S1 **S5**	**+4**	5'-G**S**G ATA TGC 3'-CAC TA**S** ACG	259±3 [+19]	275±9 [+35]	297±8 [+57]	-3
S1 **S4**	**+2**	5'-G**S**G ATA TGC 3'-CAC **S**AT ACG	259±3 [+19]	266±4 [+26]	214±5 [-26]	+71
S2 **S5**	**+1**	5'-GTG A**S**A TGC 3'-CAC TA**S** ACG	**265±6 [+25]**	**275±9 [+35]**	**231±9 [-9]**	**+69**
S2 **S4**	**-1**	5'-GTG A**S**A TGC 3'-CAC **S**AT ACG	265±6 [+25]	266±4 [+26]	265±4 [+25]	+26

[a] $\Delta(T^{293}\Delta S)$ is measured relative to $-T^{293}\Delta S$ for **D1**:**D4** = 240 kJ/mol. $-T^{293}\Delta S_{rec}$ = $\Delta(T^{293}\Delta S)$ (upper ON vs cDNA) + $\Delta(T^{293}\Delta S)$ (lower ON vs cDNA) - $\Delta(T^{293}\Delta S)$ (probe duplex).

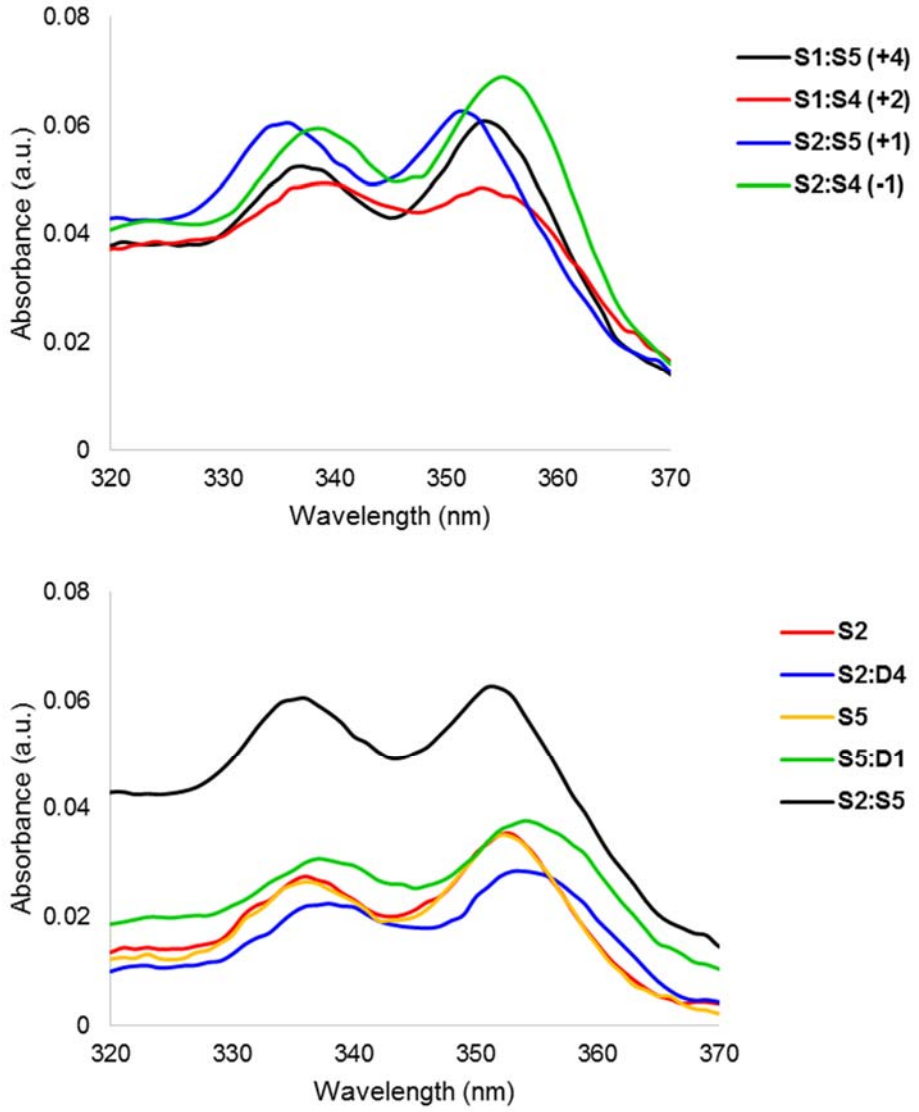

Figure S4. Absorption spectra of representative Invaders, duplexes between probe strands and cDNA, and single-stranded probes. Recorded at T = 10 °C using each strand at 1.0 μM concentration in T_m buffer.

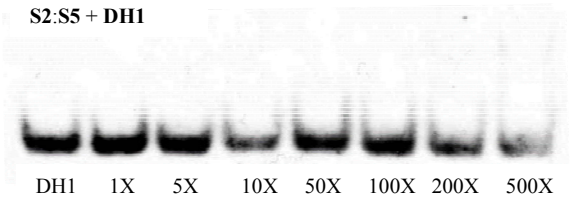

Figure S5.Representative gel electrophoretogram from experiments in which target **DH1** (34.4 nM) was annealed together with **S2**:**S5** (variable fold molar excess) at 85 °C for 15 min followed by slow cooling to room temperature over ~30 min and incubation at ambient temperature for 12-16 h. Experimental conditions otherwise as specified in Figure 4.

References

(S1) Divakar, K. J.; Mottah, A.; Reese, C. B.; Sanghvi, Y. S. *J*. *Chem*. *Soc*. *Perkin Trans*. *1* **1990**, 969.

(S2) Hendrickx, P. M. S.; Martins, J. C. *Chem*. *Cent*. *J*. **2008**, 2:20.

(S3) Donders, L. A.; Deleeuw, F. A. A. M.; Altona, C. *Magn*. *Res*. *Chem*. **1989**, *27*, 556.

(S4) (a) Diez, E.; Esteban, A.; Guilleme, J.; Bermejo, F. *J*. *Mol*. *Struct*. **1981**, *70*, 61; (b) Diez, E.; Esteban, A.; Bermejo, F.; Altona, C.; de Leeuw, F. A. A. M. *J*. Mol. *Struct*. **1984**, *125*, 49; (c) de Leeuw, F. A. A. M.; van Kampen, P.; Altona, C.; Diez, E.; Esteban, A. *J*. *Mol*. *Struct*. **1984**, *125*, 67.

(S5) Dioubankova, N. N.; Malakhov, A. D.; Stetsenko, D. A.; Gait, M. J.; Volynsky, P. E.; Efremov, R. G.; Korshun, V. A. *ChemBioChem* **2003**, *4*, 841.

(S6) Mergny, J. L.; Lacroix, L. *Oligonucleotides* **2003**, *13*, 515.

(S7) Didion, B. A.; Karmakar, S.; Guenther, D. C.; Sau, S.; Verstegen, J. P.; Hrdlicka, P. J. *ChemBioChem* **2013**, *14*, 1534.

(S8) Karmakar, S.; Anderson, B. A.; Rathje, R. L.; Andersen, S.; Jensen, T.; Nielsen, P.; Hrdlicka, P. J. *J*. *Org*. *Chem*. **2011**, *76*, 7119.

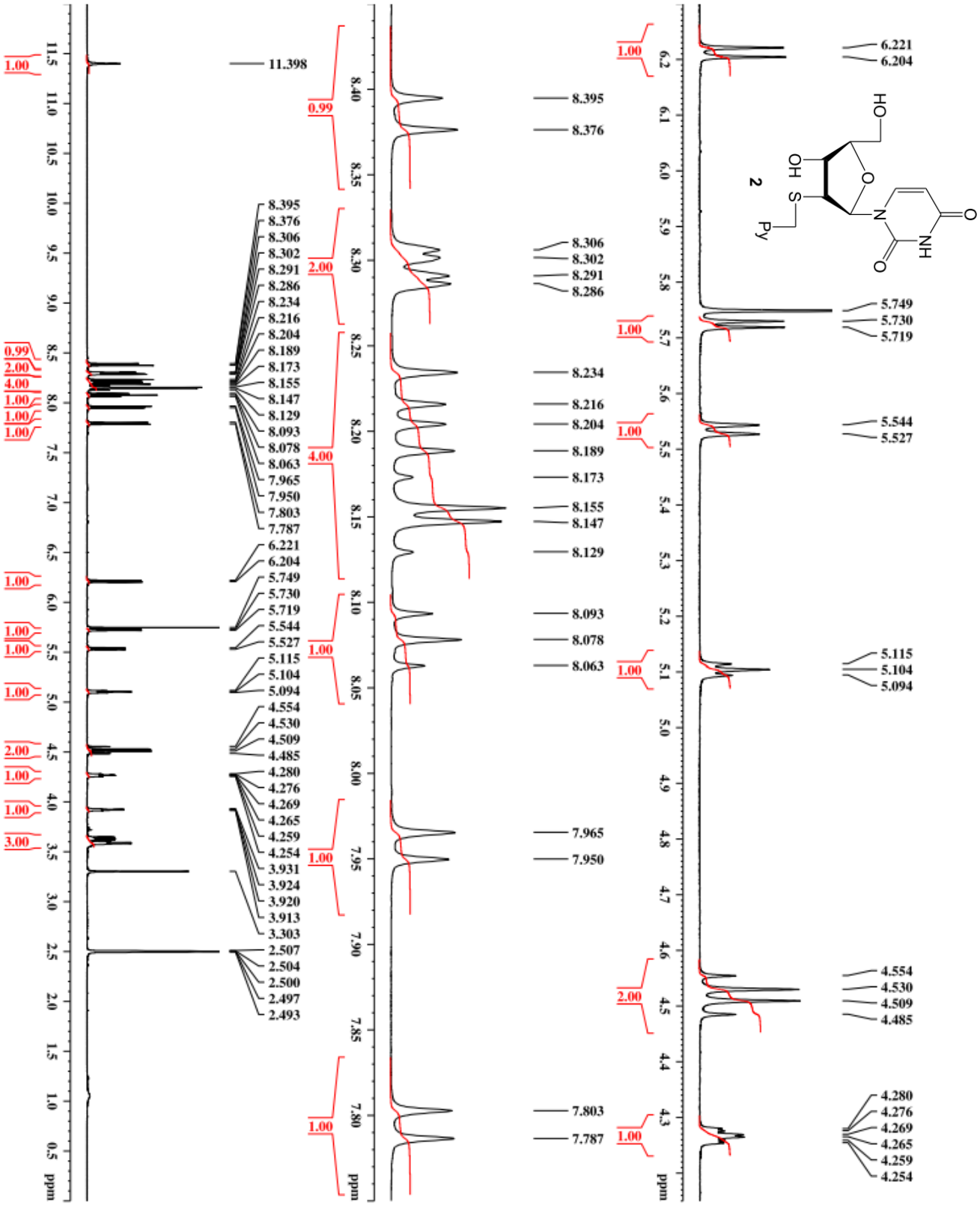
11.398
8.395
8.376
8.306
8.302
8.291
8.286
8.234
8.216
8.204
8.189
8.173
8.155
8.147
8.129
8.093
8.078
8.063
7.965
7.950
7.803
7.787
6.221
6.204
5.749
5.730
5.719
5.544
5.527
5.115
5.104
5.094
4.554
4.530
4.509
4.485
4.280
4.276
4.269
4.265
4.259
4.254
3.931
3.924
3.920
3.913
3.303
2.507
2.504
2.500
2.497
2.493
HO
OH
O
S
N
Py
2
NH
O
O
ppm

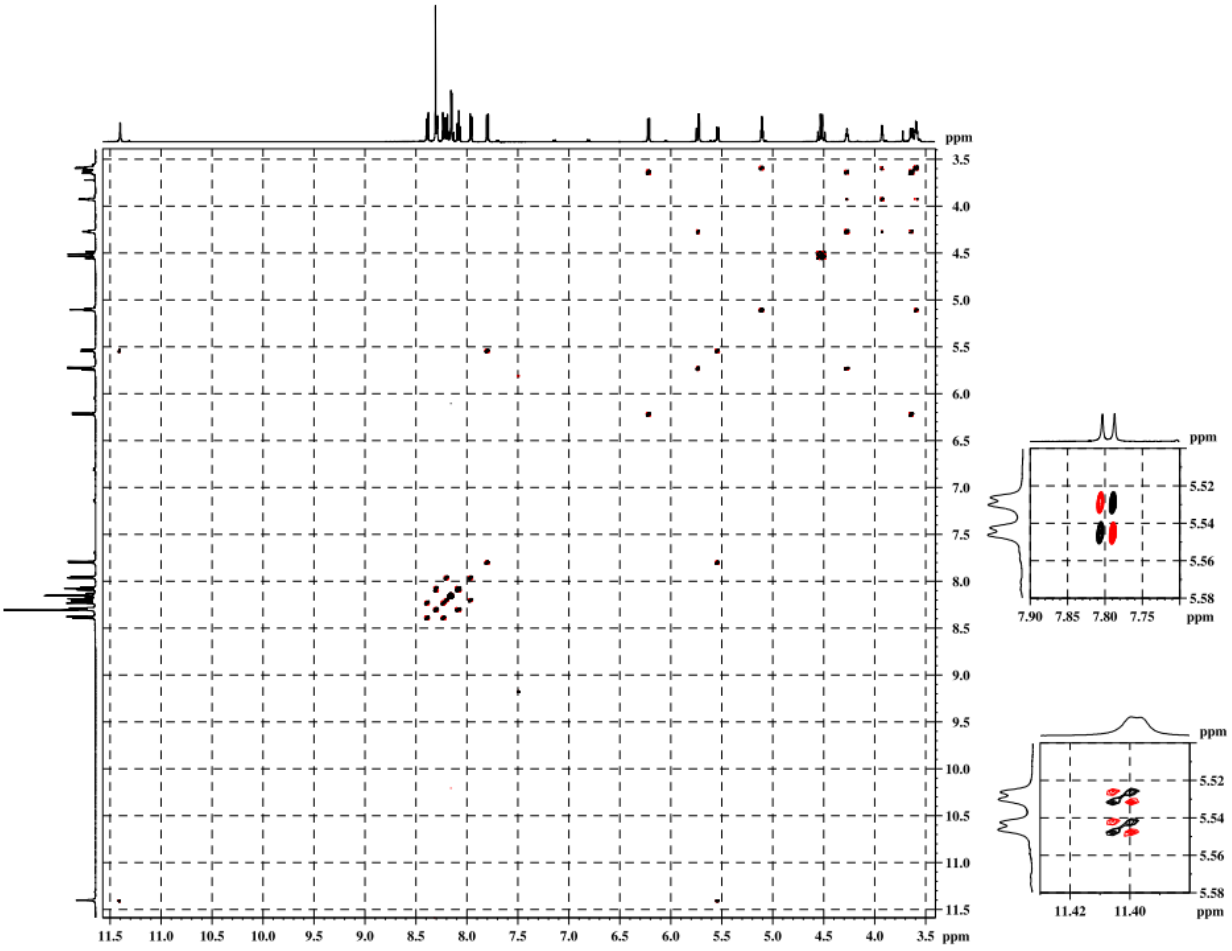
ppm
3.5
4.0
4.5
5.0
5.5
6.0
6.5
7.0
7.5
8.0
8.5
9.0
9.5
10.0
10.5
11.0
11.5
11.5 11.0 10.5 10.0 9.5 9.0 8.5 8.0 7.5 7.0 6.5 6.0 5.5 5.0 4.5 4.0 3.5 ppm
ppm
5.52
5.54
5.56
5.58
7.90 7.85 7.80 7.75 ppm
ppm
5.52
5.54
5.56
5.58
11.42 11.40 ppm

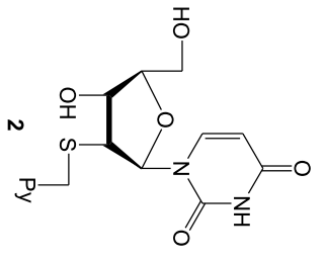
HO
OH
O
2
S
N
O
Py
NH
O

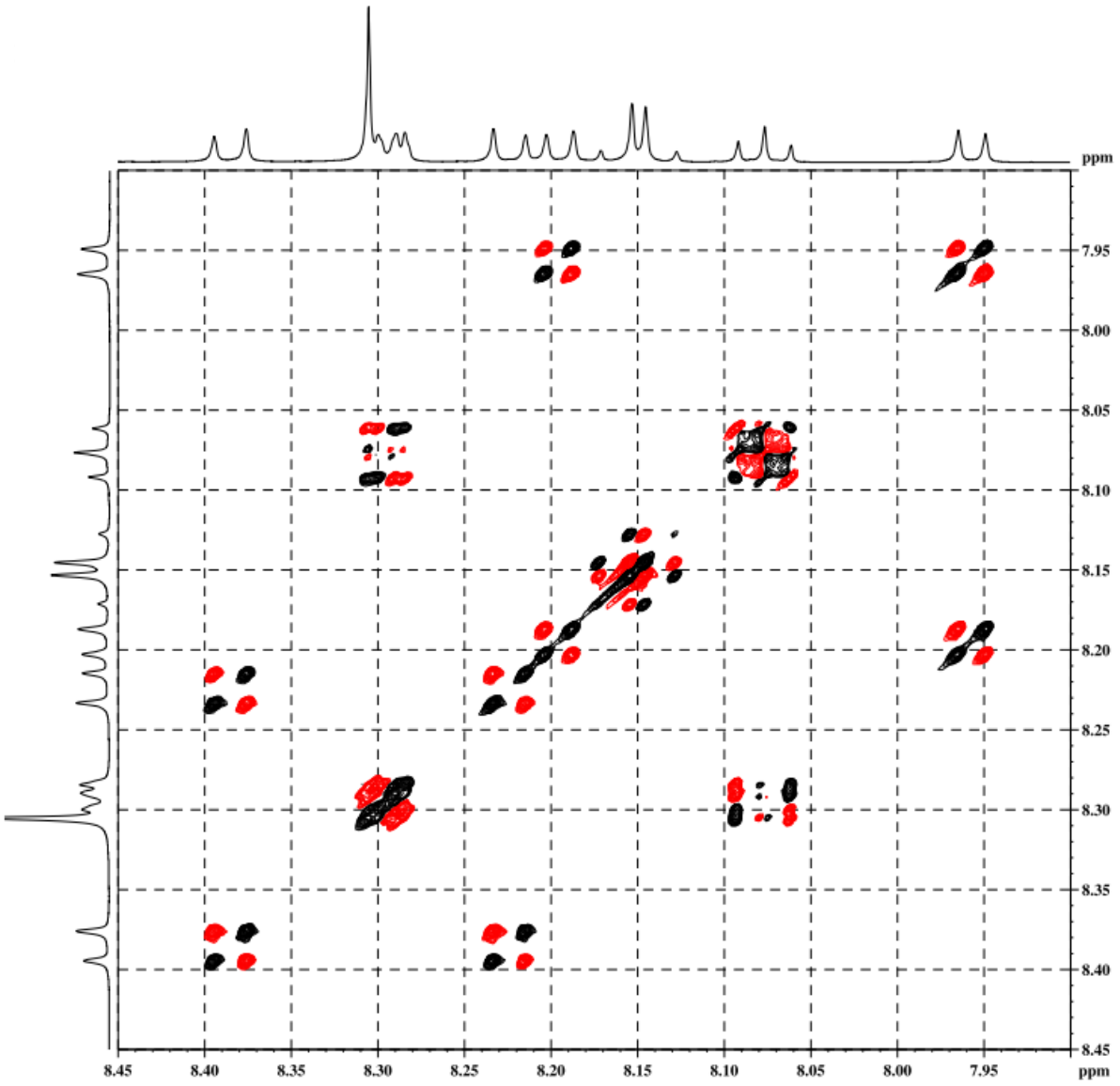
ppm
7.95
8.00
8.05
8.10
8.15
8.20
8.25
8.30
8.35
8.40
8.45
8.45
8.40
8.35
8.30
8.25
8.20
8.15
8.10
8.05
8.00
7.95
ppm

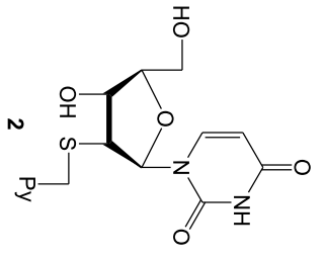
HO
O
OH
S
2
Py
N
O
NH
O

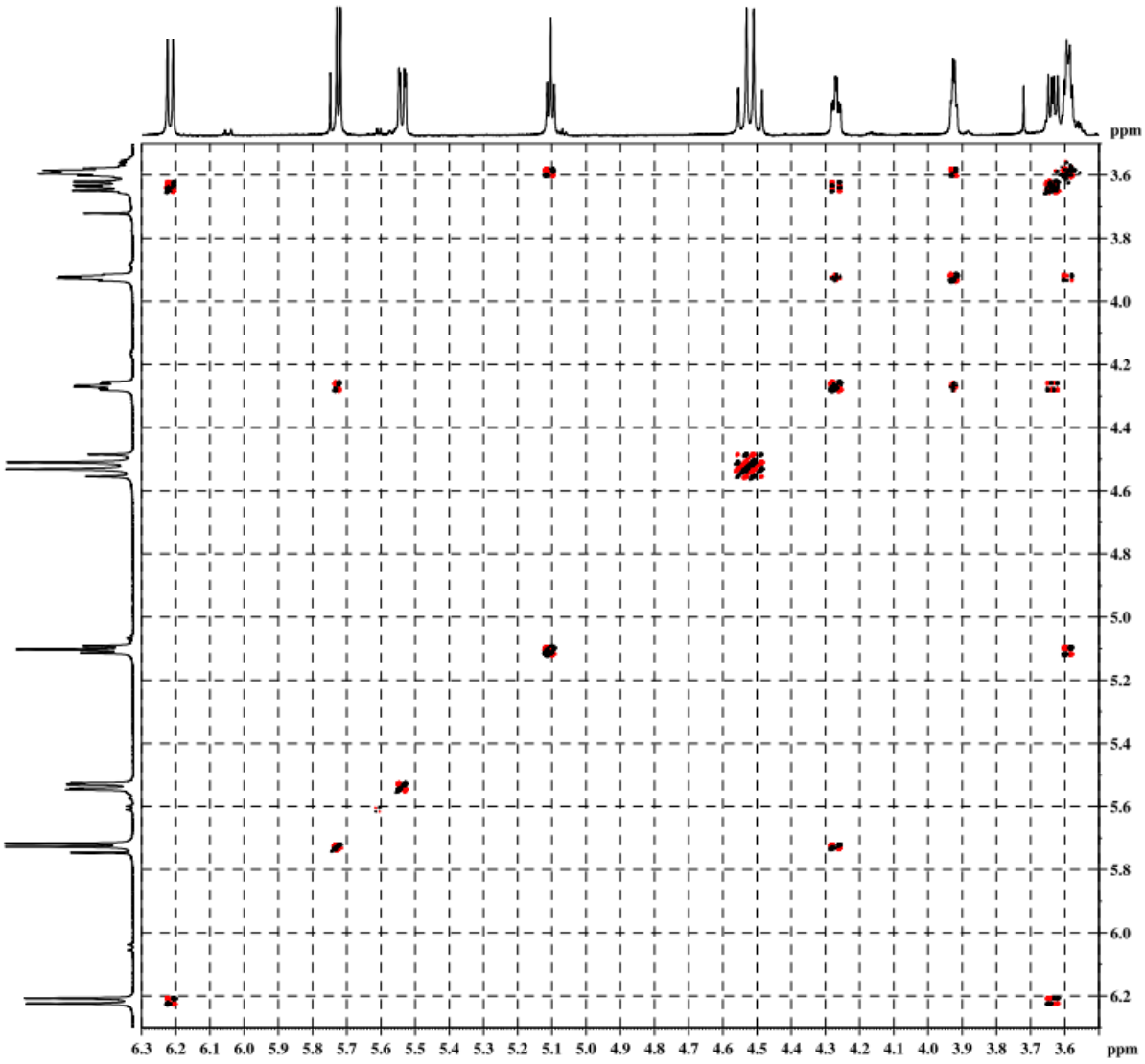
ppm
3.6
3.8
4.0
4.2
4.4
4.6
4.8
5.0
5.2
5.4
5.6
5.8
6.0
6.2
6.3 6.2 6.1 6.0 5.9 5.8 5.7 5.6 5.5 5.4 5.3 5.2 5.1 5.0 4.9 4.8 4.7 4.6 4.5 4.4 4.3 4.2 4.1 4.0 3.9 3.8 3.7 3.6
ppm

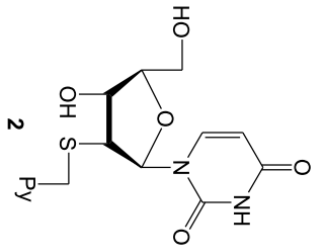
HO
OH
O
2
S
N
O
Py
NH
O

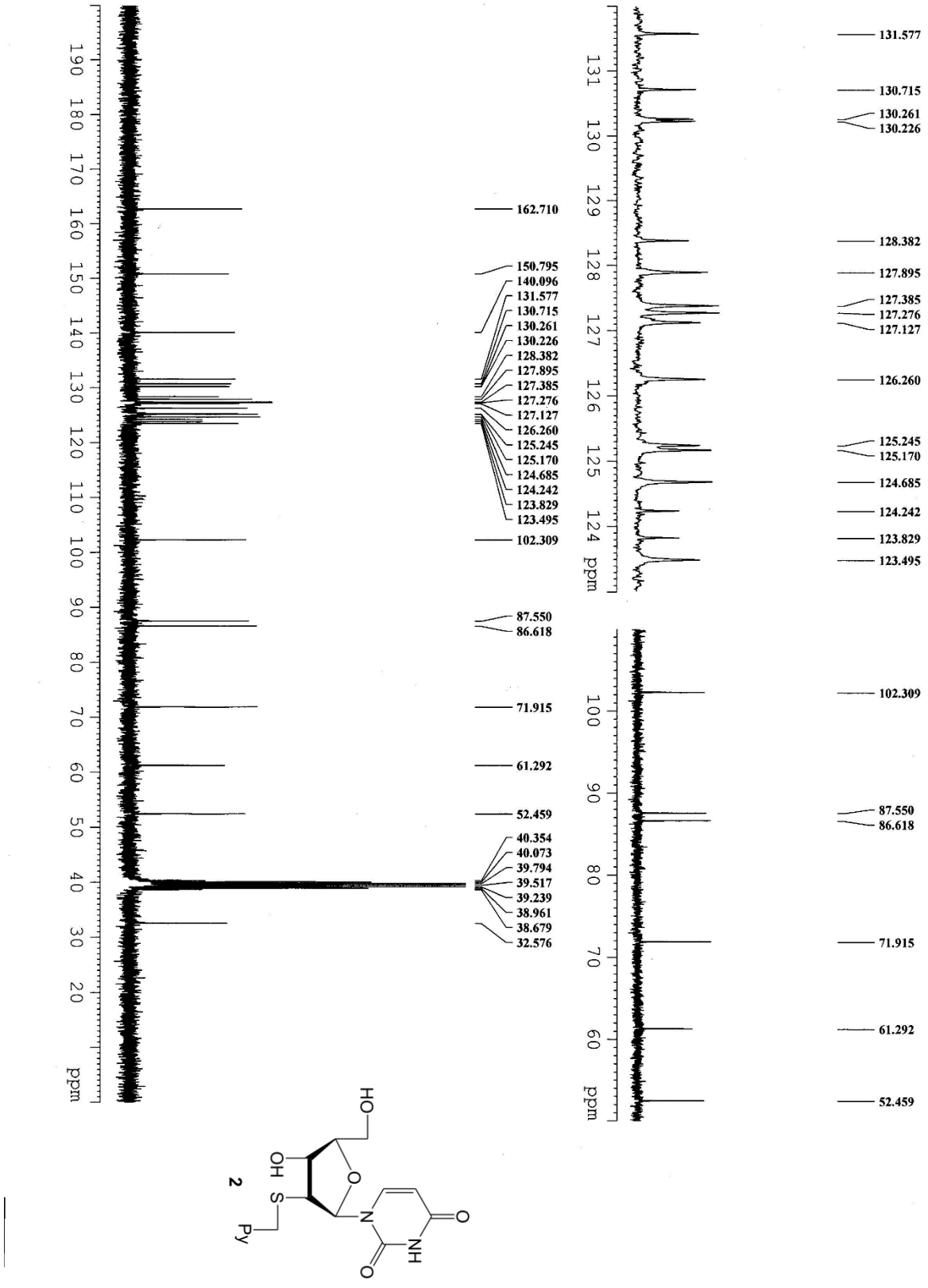
162.710
150.795
140.096
131.577
130.715
130.261
130.226
128.382
127.895
127.385
127.276
127.127
126.260
125.245
125.170
124.685
124.242
123.829
123.495
102.309
87.550
86.618
71.915
61.292
52.459
40.354
40.073
39.794
39.517
39.239
38.961
38.679
32.576
ppm
131.577
130.715
130.261
130.226
128.382
127.895
127.385
127.276
127.127
126.260
125.245
125.170
124.685
124.242
123.829
123.495
102.309
87.550
86.618
71.915
61.292
52.459
HO
OH
S
Py
2
O
N
NH
O
O

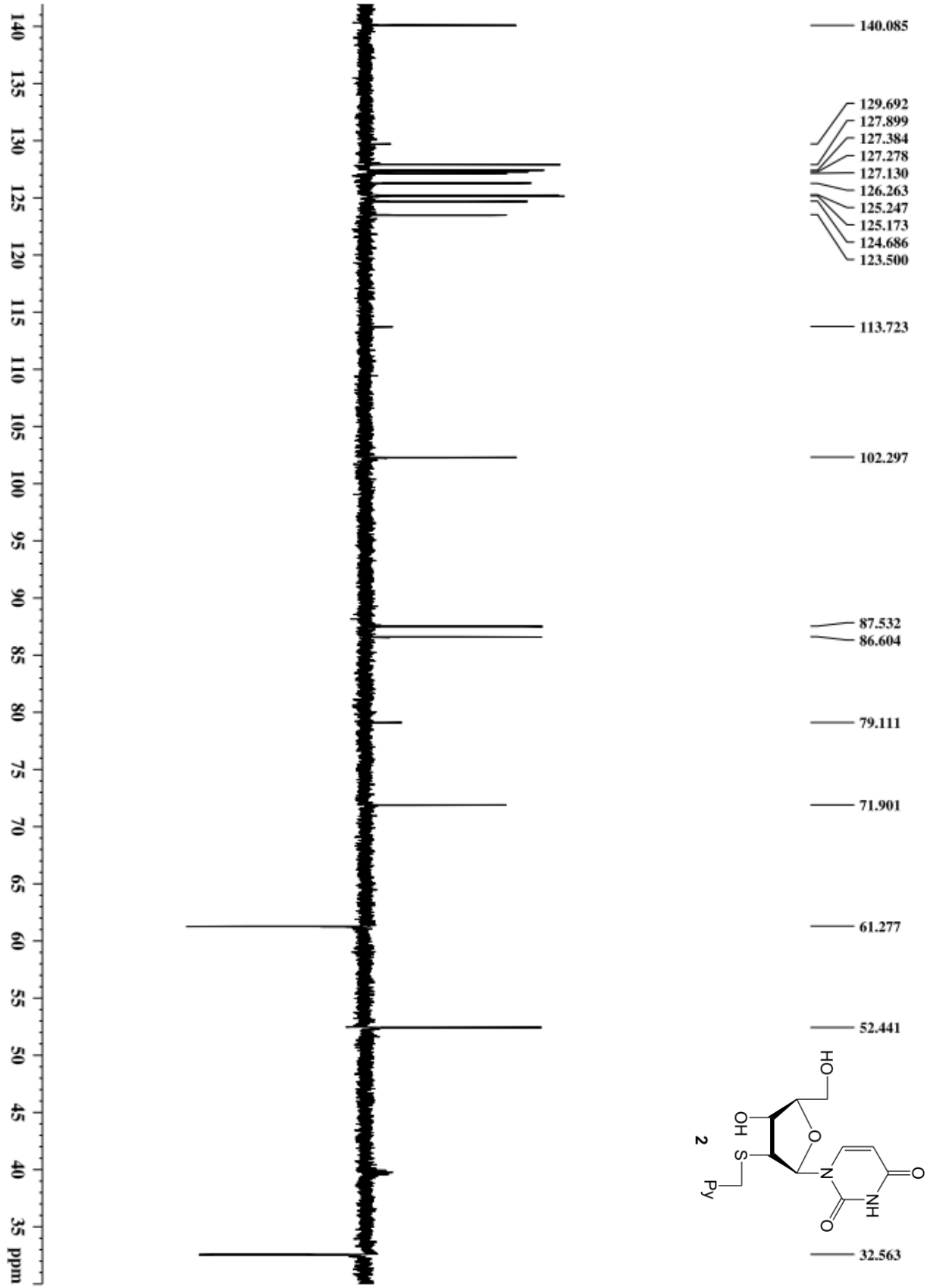
140.085
129.692
127.899
127.384
127.278
127.130
126.263
125.247
125.173
124.686
123.500
113.723
102.297
87.532
86.604
79.111
71.901
61.277
52.441
32.563
140 135 130 125 120 115 110 105 100 95 90 85 80 75 70 65 60 55 50 45 40 35 ppm
HO
O
OH
S
2
Py
N
NH
O
O

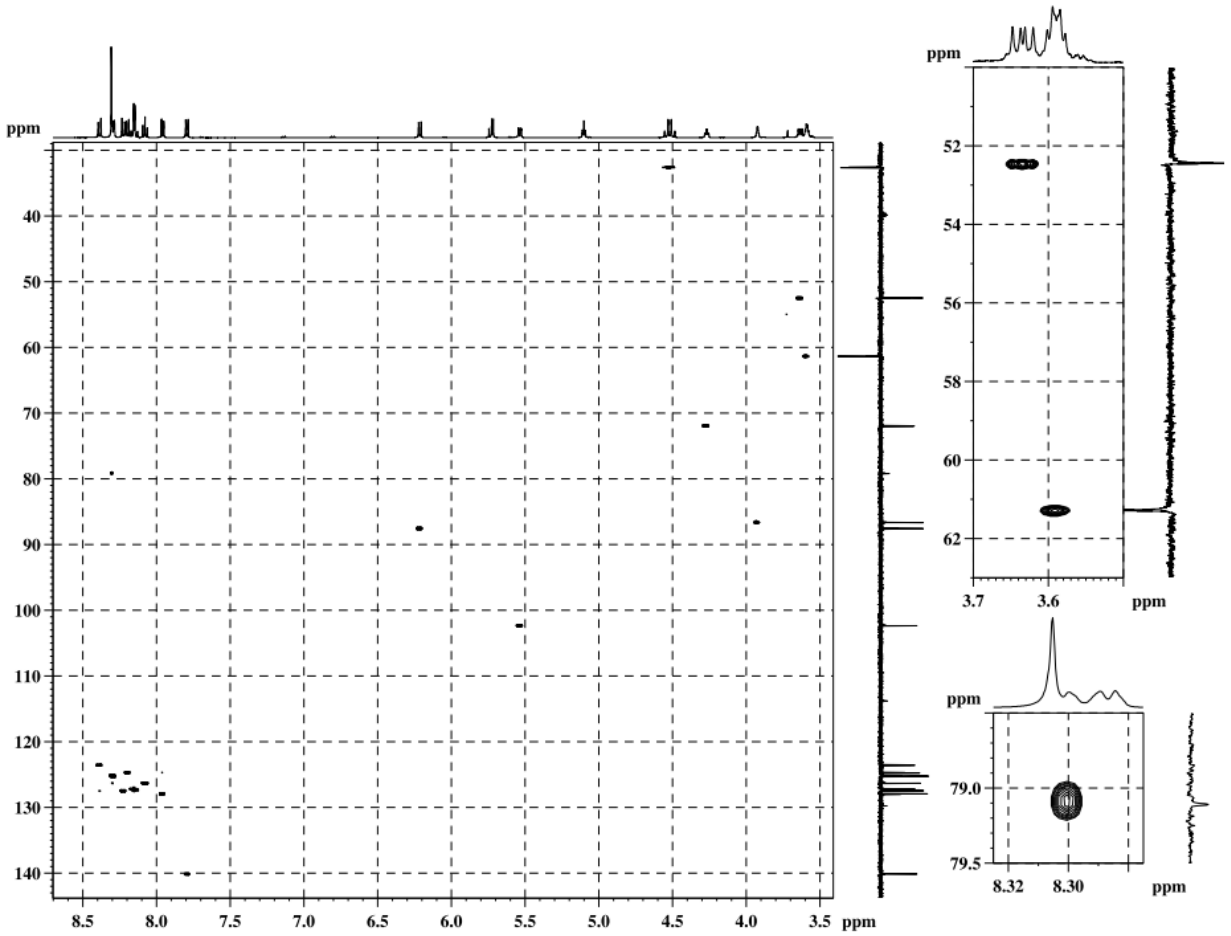
ppm
40
50
60
70
80
90
100
110
120
130
140
8.5
8.0
7.5
7.0
6.5
6.0
5.5
5.0
4.5
4.0
3.5
ppm
ppm
52
54
56
58
60
62
3.7
3.6
ppm
ppm
79.0
79.5
8.32
8.30
ppm

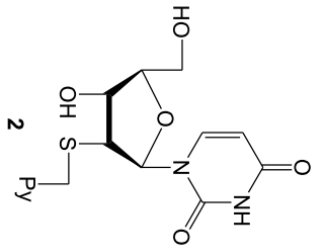
HO
OH
S
2
Py
O
N
O
NH
O

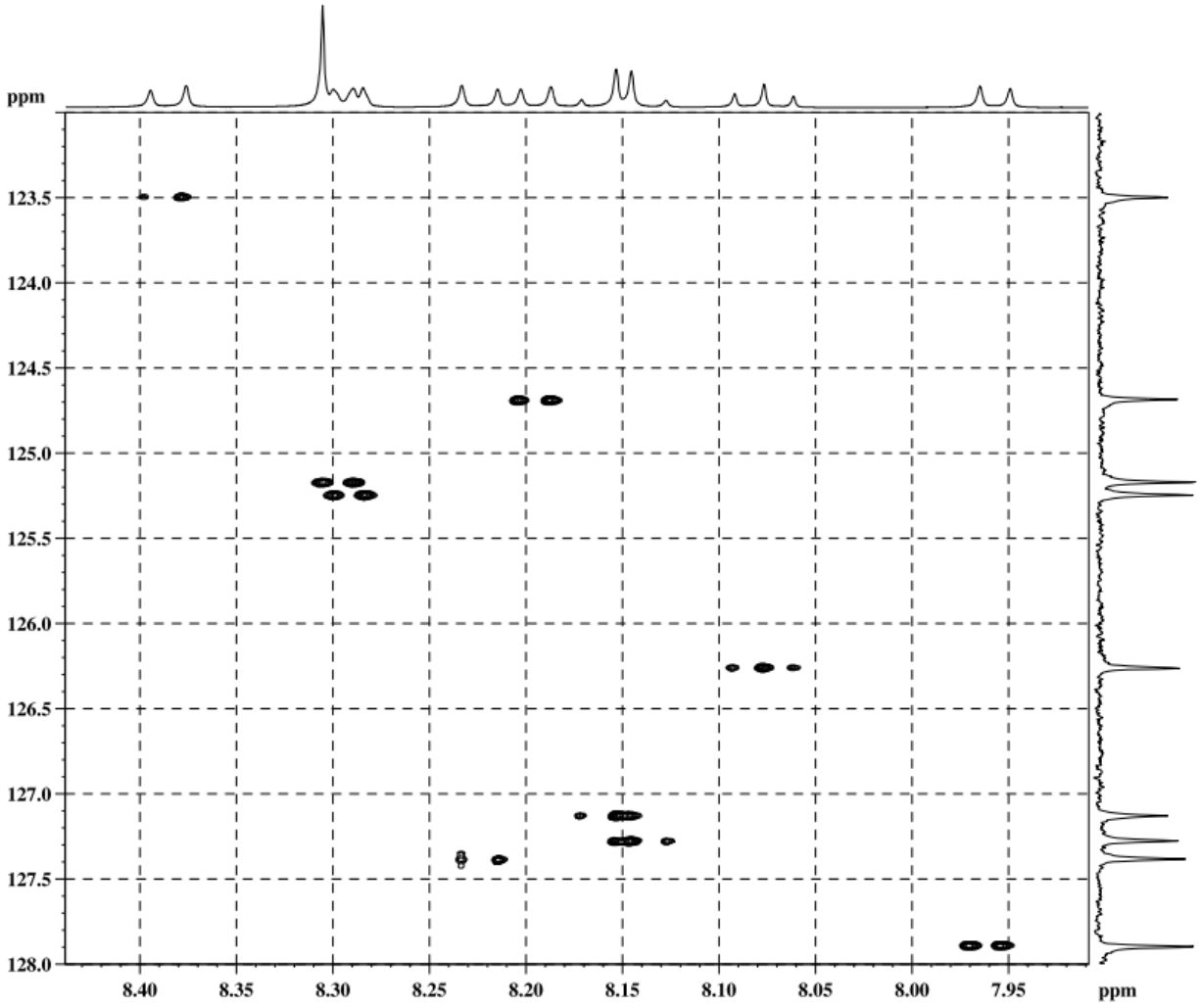
ppm
123.5
124.0
124.5
125.0
125.5
126.0
126.5
127.0
127.5
128.0
8.40
8.35
8.30
8.25
8.20
8.15
8.10
8.05
8.00
7.95
ppm

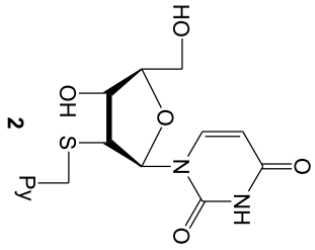
HO
OH
O
2
S
N
O
Py
NH
O

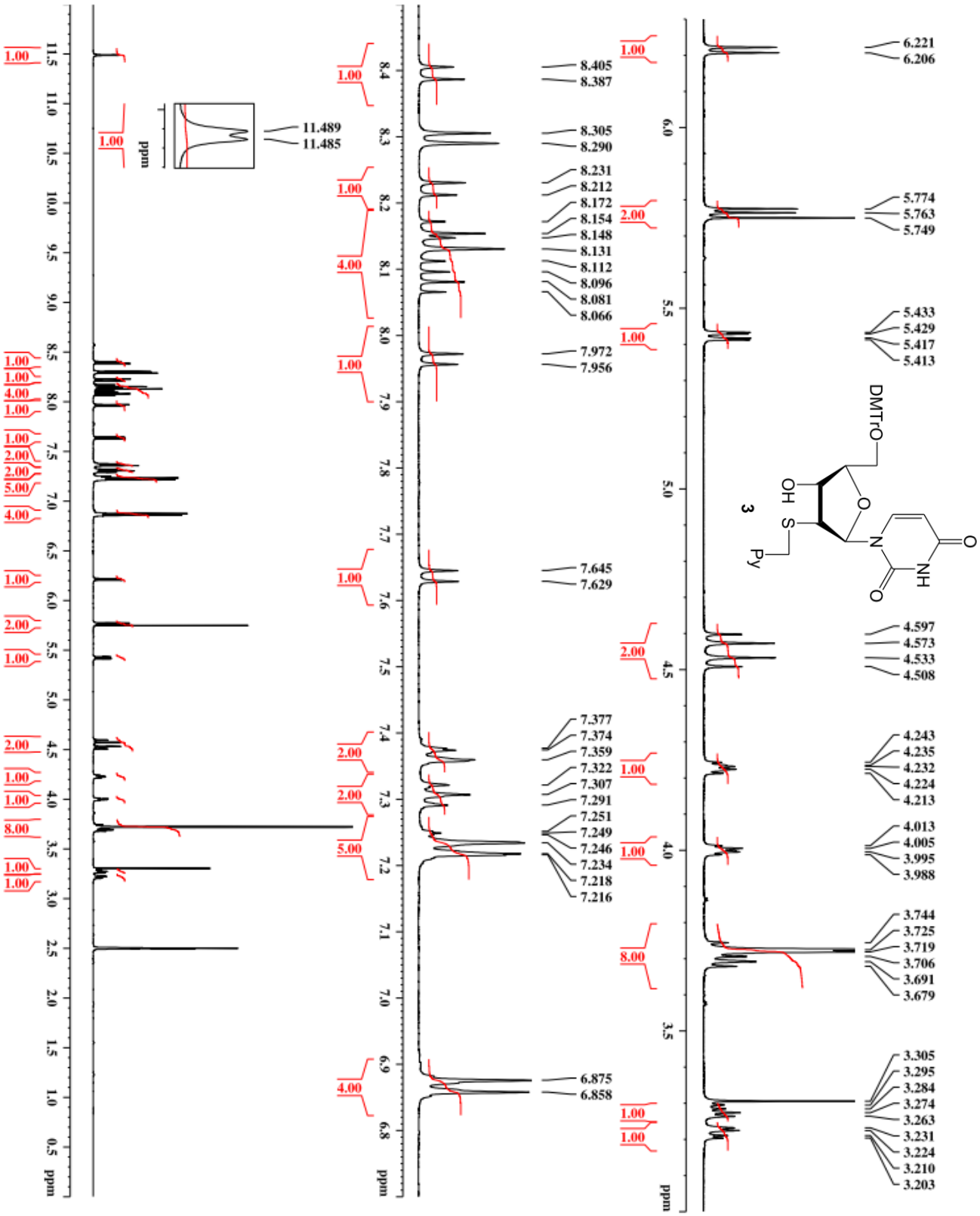
DMTrO
OH
S
Py
3
O
N
NH
O
O
6.221
6.206
5.774
5.763
5.749
5.433
5.429
5.417
5.413
4.597
4.573
4.533
4.508
4.243
4.235
4.232
4.224
4.213
4.013
4.005
3.995
3.988
3.744
3.725
3.719
3.706
3.691
3.679
3.305
3.295
3.284
3.274
3.263
3.231
3.224
3.210
3.203
8.405
8.387
8.305
8.290
8.231
8.212
8.172
8.154
8.148
8.131
8.112
8.096
8.081
8.066
7.972
7.956
7.645
7.629
7.377
7.374
7.359
7.322
7.307
7.291
7.251
7.249
7.246
7.234
7.218
7.216
6.875
6.858
11.489
11.485
ppm

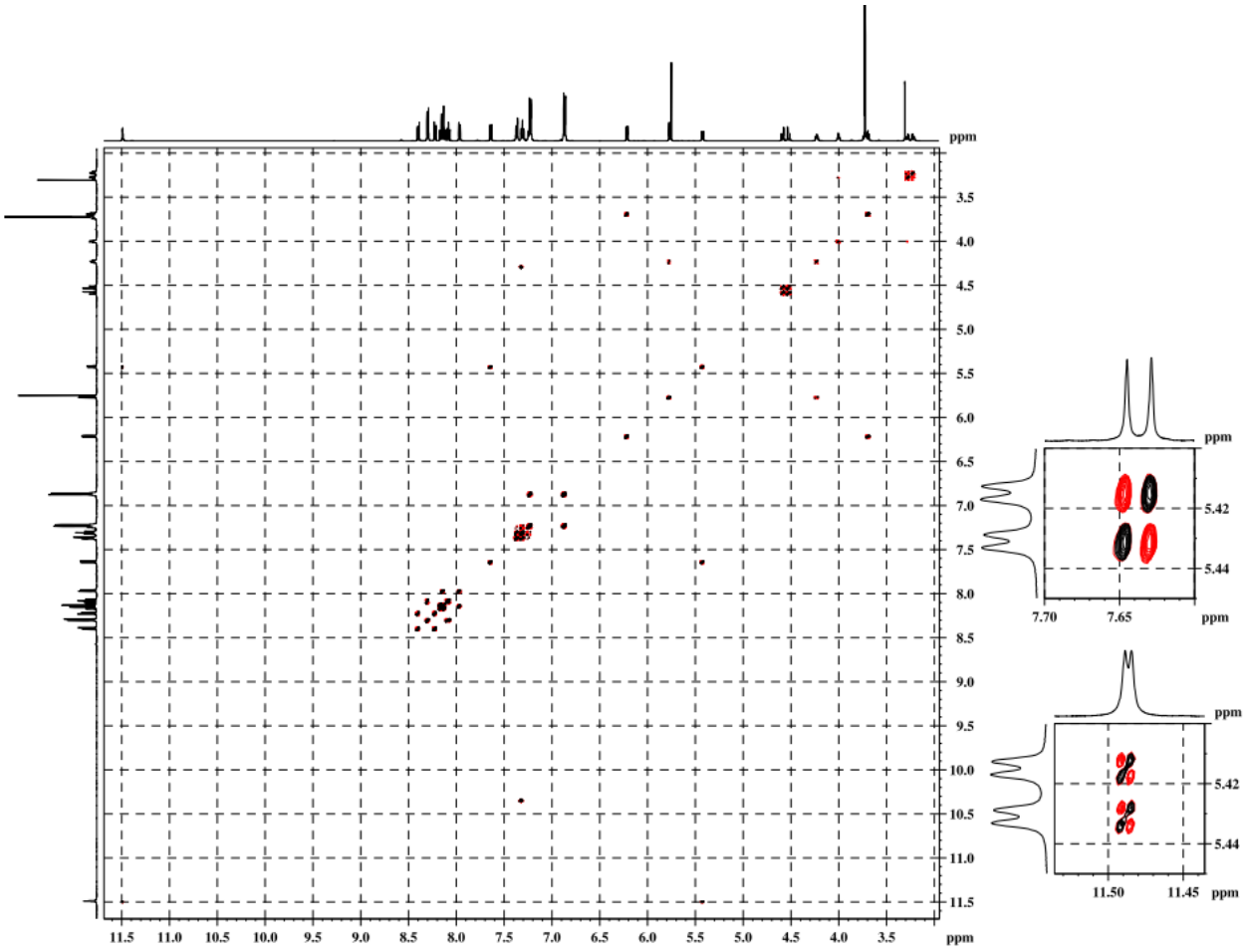
ppm
3.5
4.0
4.5
5.0
5.5
6.0
6.5
7.0
7.5
8.0
8.5
9.0
9.5
10.0
10.5
11.0
11.5
11.5 11.0 10.5 10.0 9.5 9.0 8.5 8.0 7.5 7.0 6.5 6.0 5.5 5.0 4.5 4.0 3.5 ppm
ppm
5.42
5.44
7.70
7.65
ppm
ppm
5.42
5.44
11.50
11.45
ppm

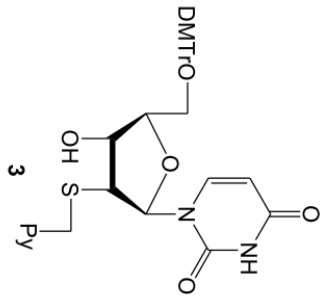
DMTrO
O
OH
3
S
Py
N
NH
O
O

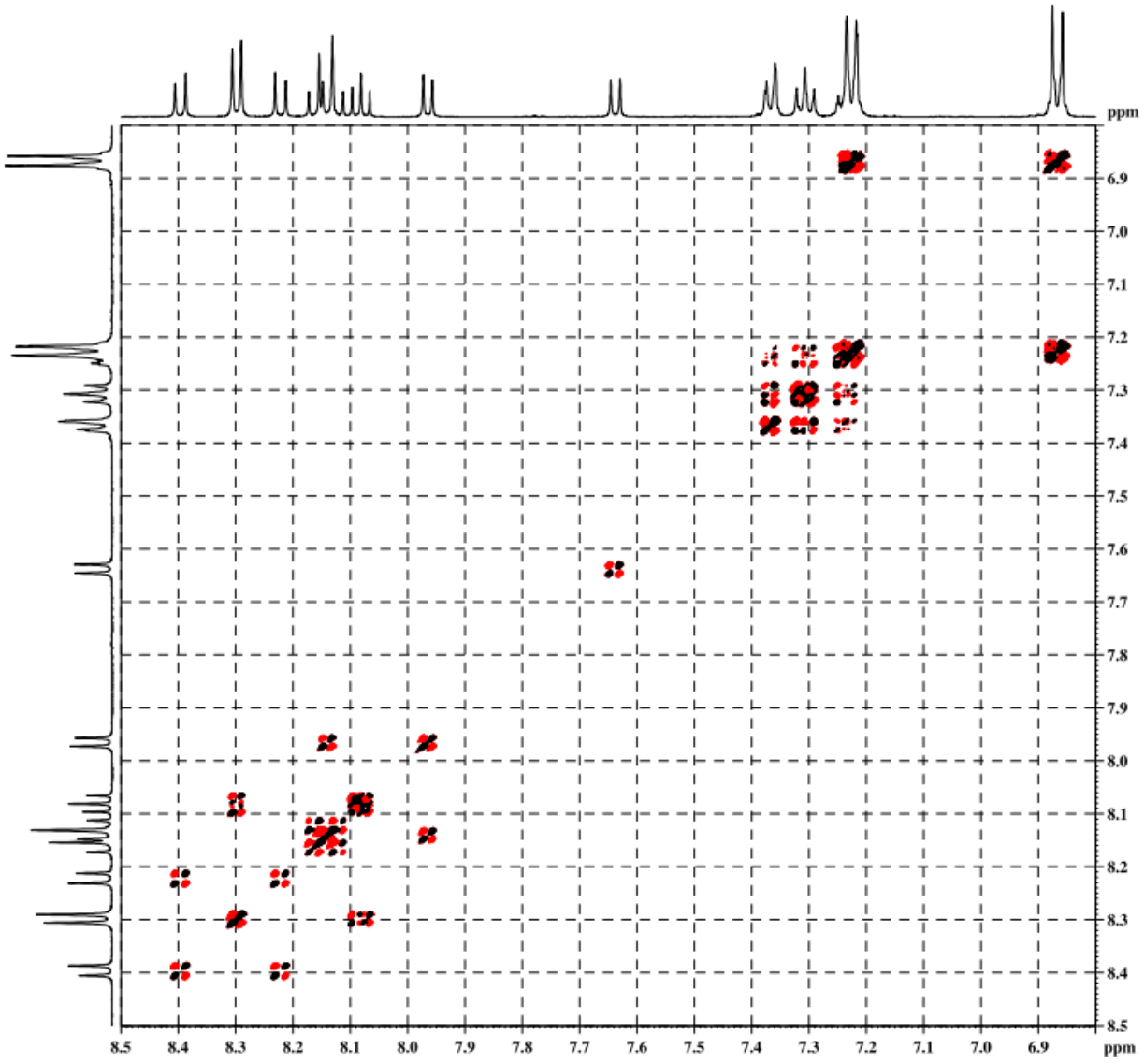
ppm
6.9
7.0
7.1
7.2
7.3
7.4
7.5
7.6
7.7
7.8
7.9
8.0
8.1
8.2
8.3
8.4
8.5
8.5 8.4 8.3 8.2 8.1 8.0 7.9 7.8 7.7 7.6 7.5 7.4 7.3 7.2 7.1 7.0 6.9 ppm

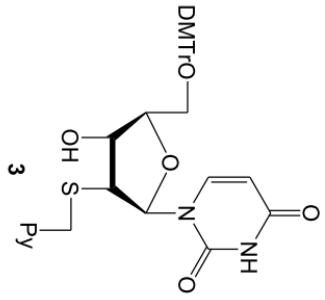
DMTrO
OH
3
S
Py
O
N
NH
O
O

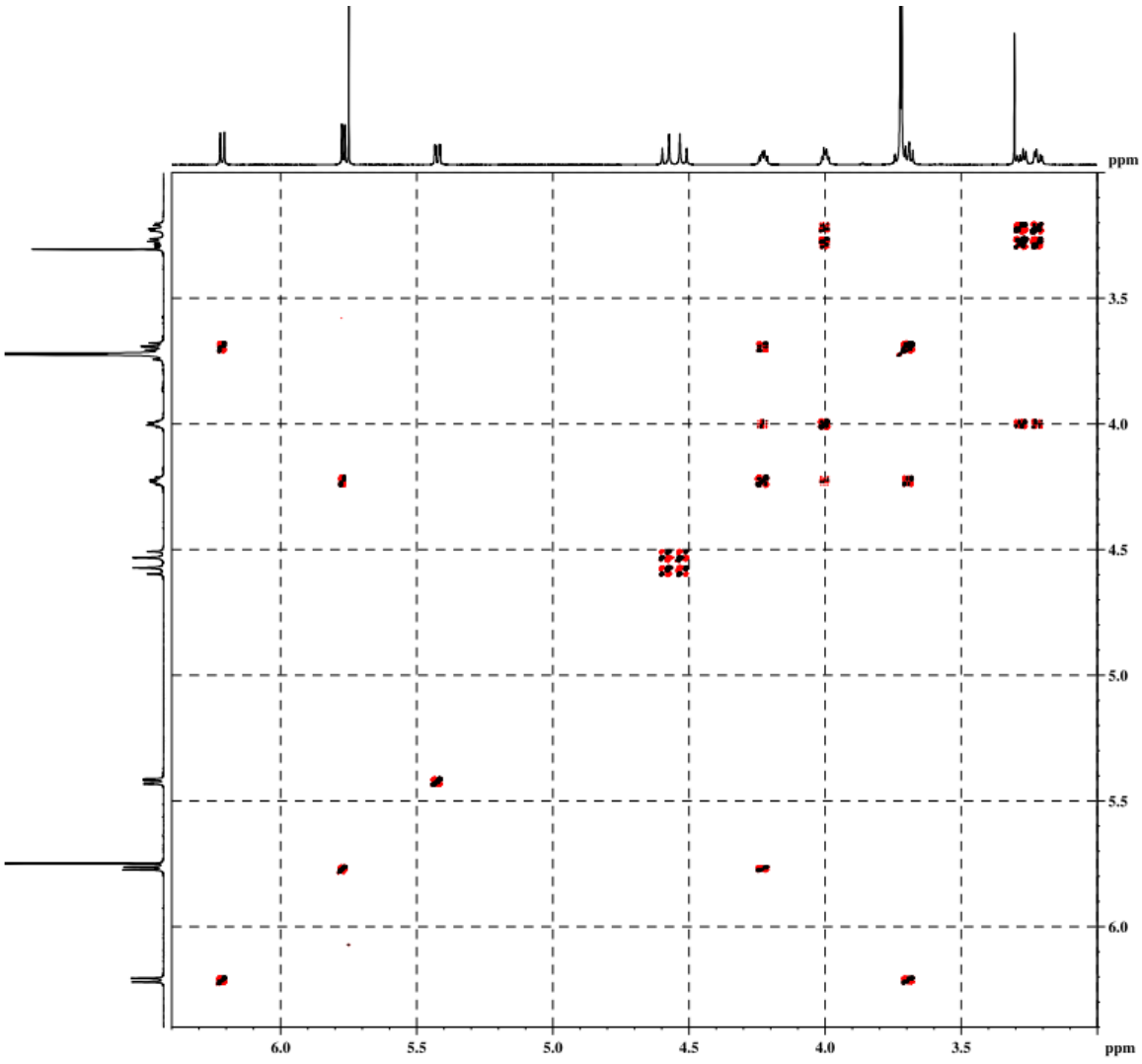
ppm
3.5
4.0
4.5
5.0
5.5
6.0
6.0
5.5
5.0
4.5
4.0
3.5
ppm

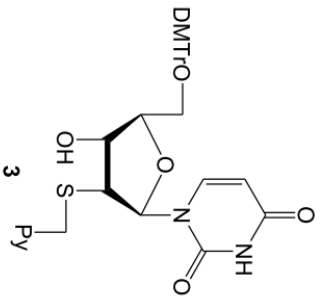
DMTrO
OH
3
S
Py
O
N
NH
O
O

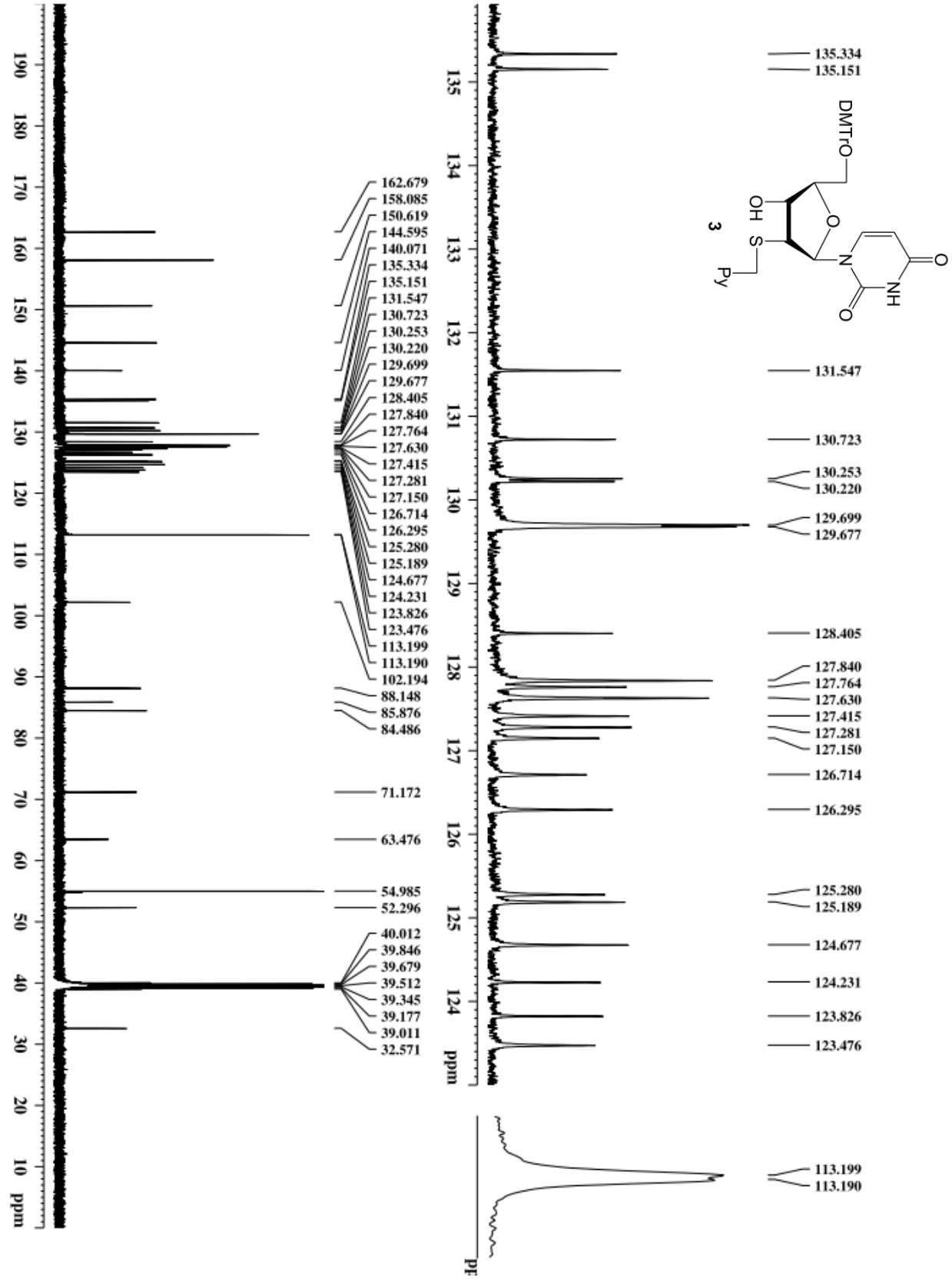
DMTrO
OH
S
Py
3
O
N
NH
O
O
135.334
135.151
131.547
130.723
130.253
130.220
129.699
129.677
128.405
127.840
127.764
127.630
127.415
127.281
127.150
126.714
126.295
125.280
125.189
124.677
124.231
123.826
123.476
113.199
113.190
162.679
158.085
150.619
144.595
140.071
135.334
135.151
131.547
130.723
130.253
130.220
129.699
129.677
128.405
127.840
127.764
127.630
127.415
127.281
127.150
126.714
126.295
125.280
125.189
124.677
124.231
123.826
123.476
113.199
113.190
102.194
88.148
85.876
84.486
71.172
63.476
54.985
52.296
40.012
39.846
39.679
39.512
39.345
39.177
39.011
32.571
ppm

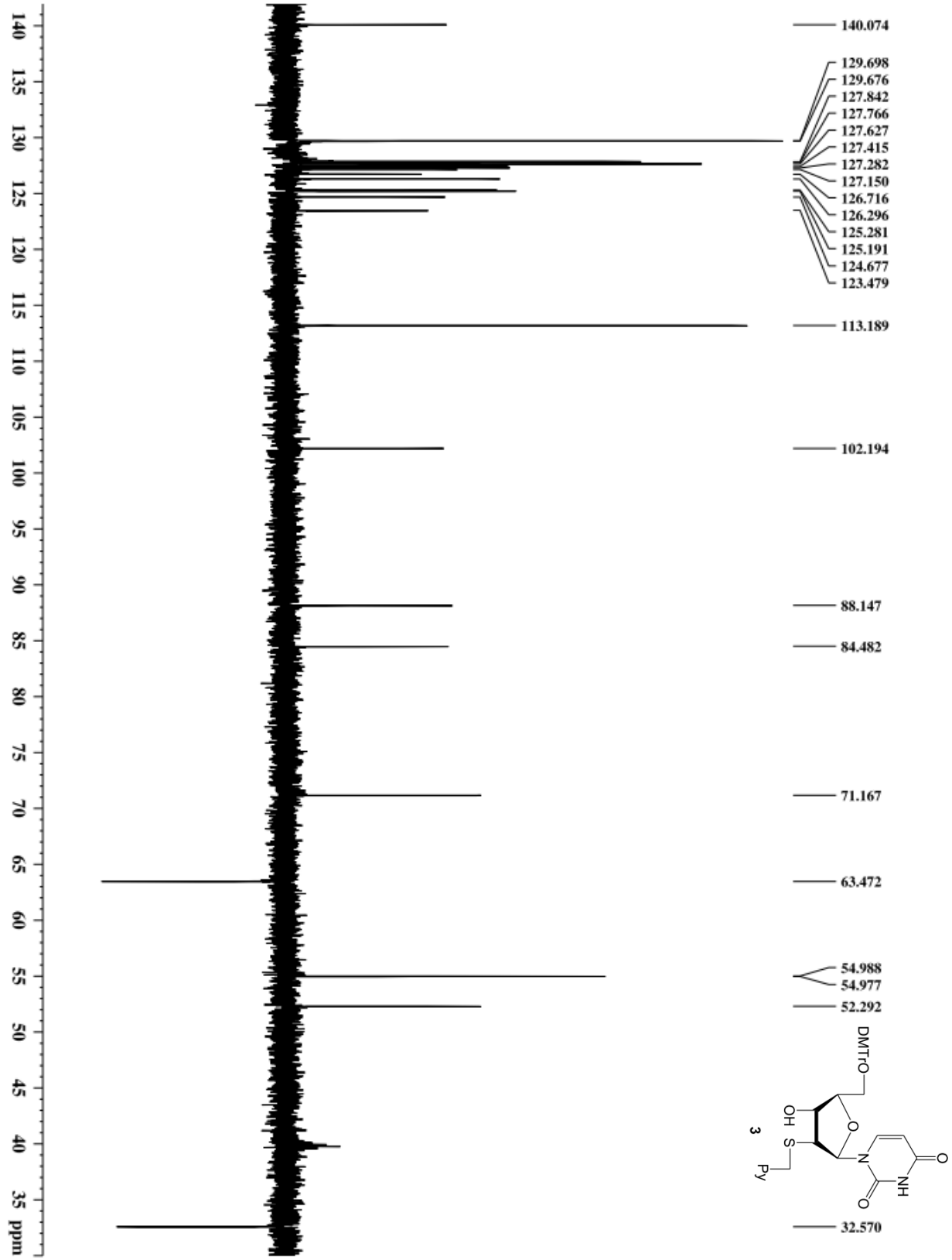
140.074
129.698
129.676
127.842
127.766
127.627
127.415
127.282
127.150
126.716
126.296
125.281
125.191
124.677
123.479
113.189
102.194
88.147
84.482
71.167
63.472
54.988
54.977
52.292
32.570
DMTrO
OH
3
S
Py
O
N
NH
O
O
140 135 130 125 120 115 110 105 100 95 90 85 80 75 70 65 60 55 50 45 40 35 ppm

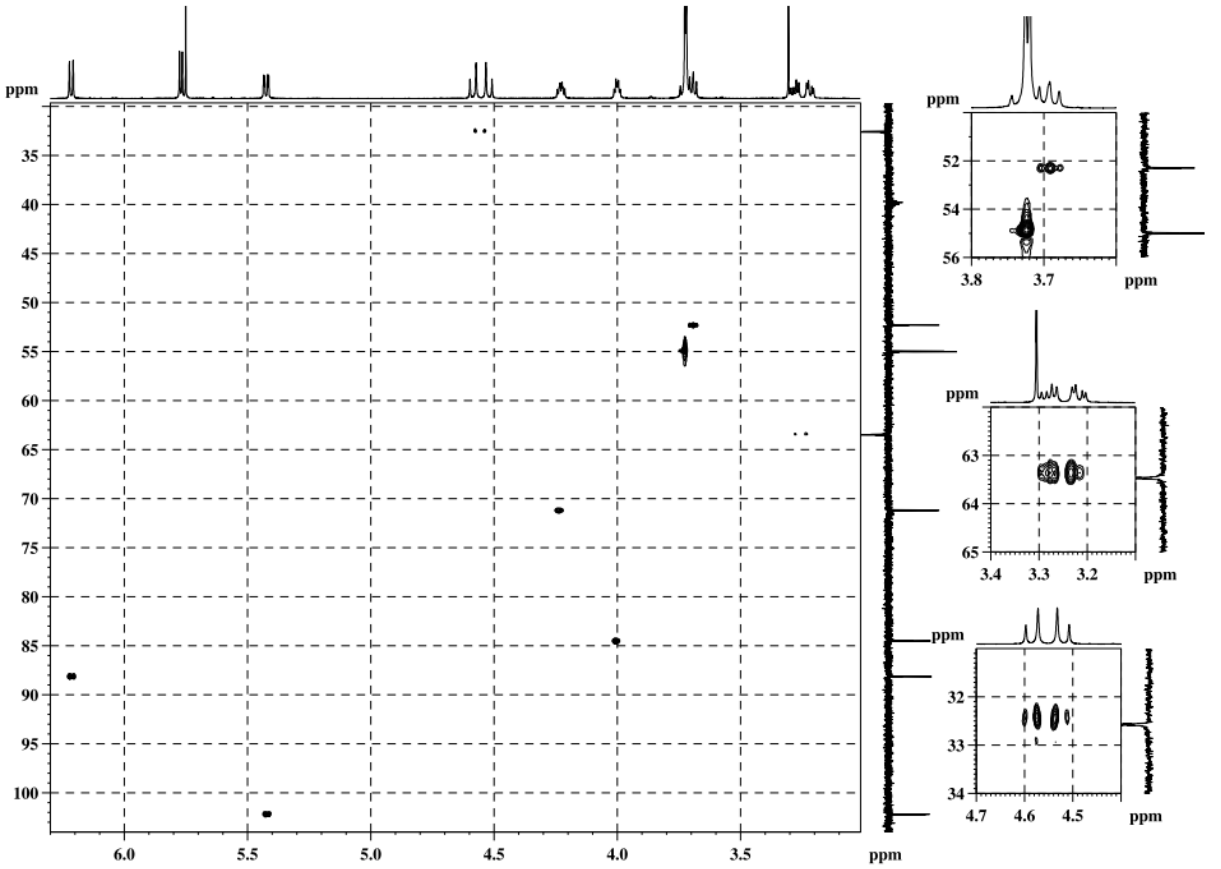
ppm
35
40
45
50
55
60
65
70
75
80
85
90
95
100
6.0
5.5
5.0
4.5
4.0
3.5
ppm
52
54
56
3.8
3.7
63
64
65
3.4
3.3
3.2
32
33
34
4.7
4.6
4.5

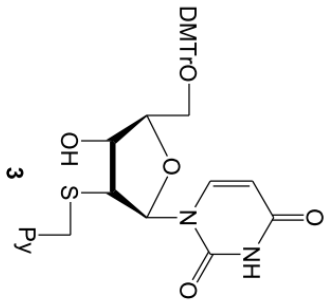
DMTrO
OH
3
S
Py
O
N
NH
O
O

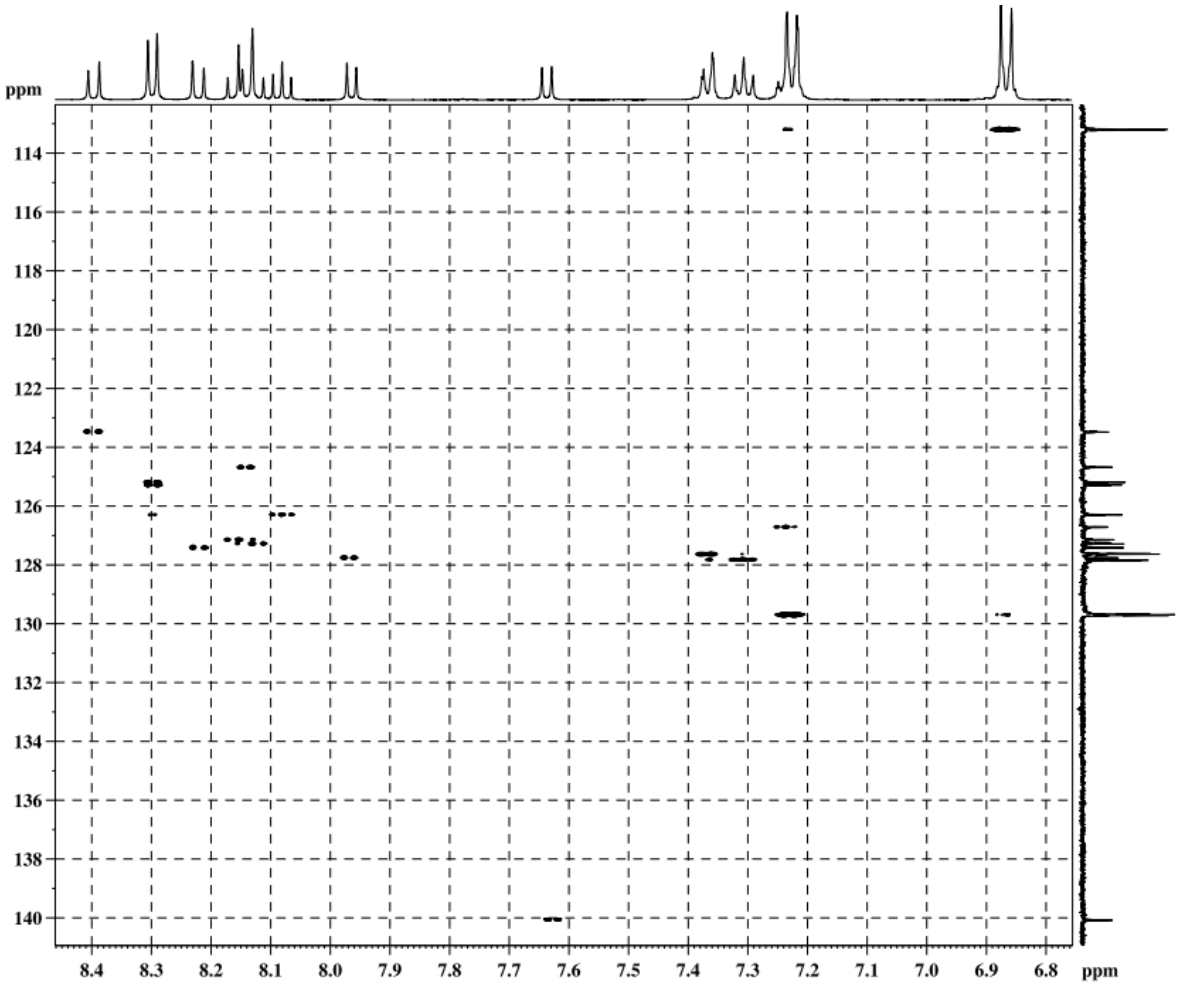
ppm
114
116
118
120
122
124
126
128
130
132
134
136
138
140
8.4
8.3
8.2
8.1
8.0
7.9
7.8
7.7
7.6
7.5
7.4
7.3
7.2
7.1
7.0
6.9
6.8
ppm

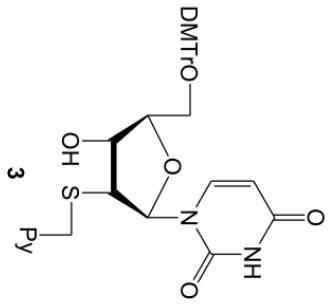
DMTrO
OH
3
S
Py
O
N
NH
O
O

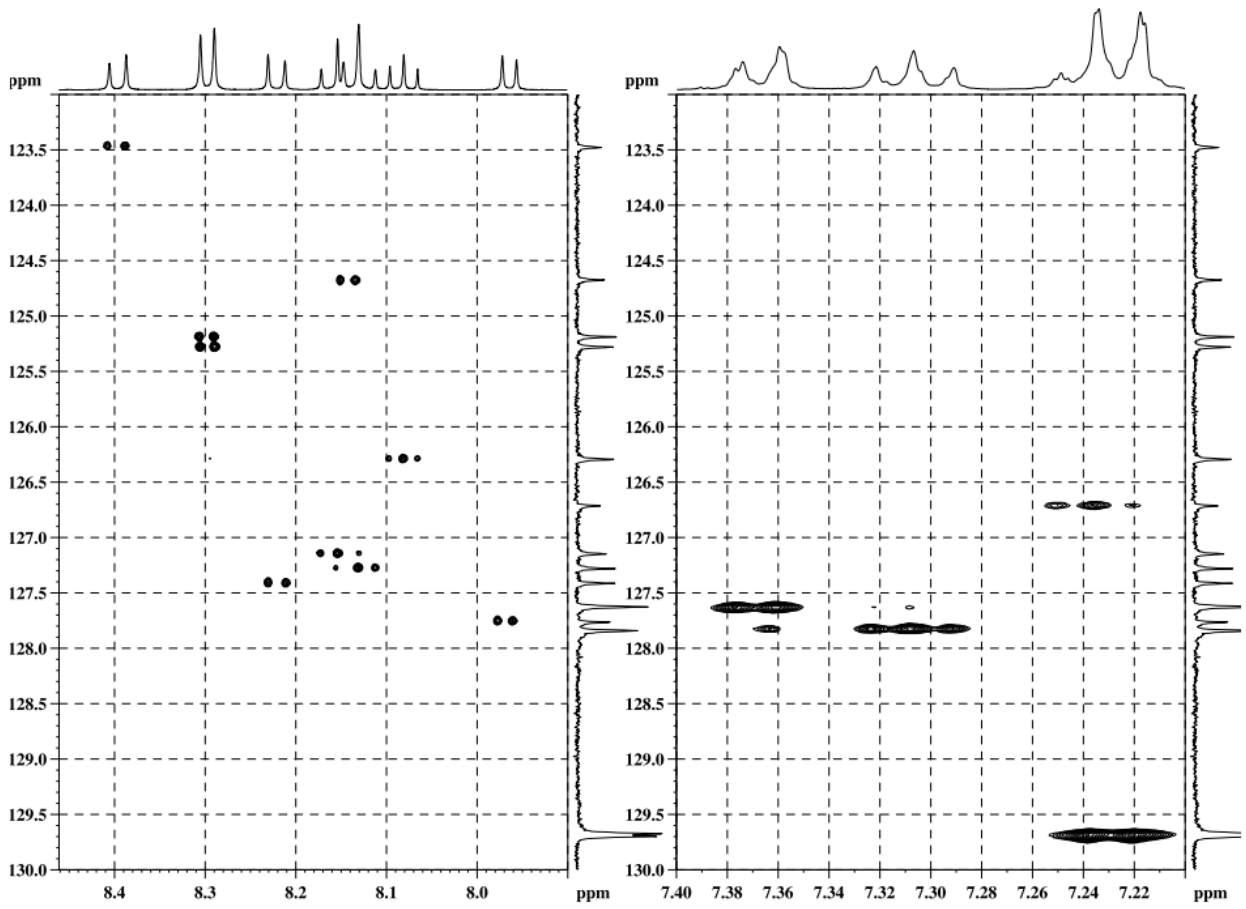
ppm
123.5
124.0
124.5
125.0
125.5
126.0
126.5
127.0
127.5
128.0
128.5
129.0
129.5
130.0
8.4
8.3
8.2
8.1
8.0
ppm
7.40
7.38
7.36
7.34
7.32
7.30
7.28
7.26
7.24
7.22
ppm

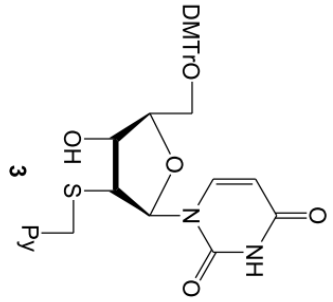
DMTrO
OH
3
S
Py
O
N
NH
O
O

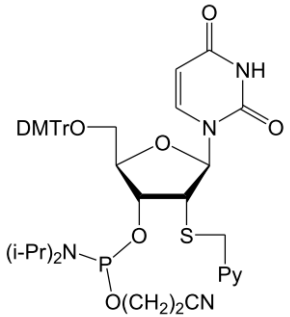
O
NH
DMTrO
N
O
O
O
S
(i-Pr)2N
P
Py
O(CH2)2CN

4


150.886
149.908

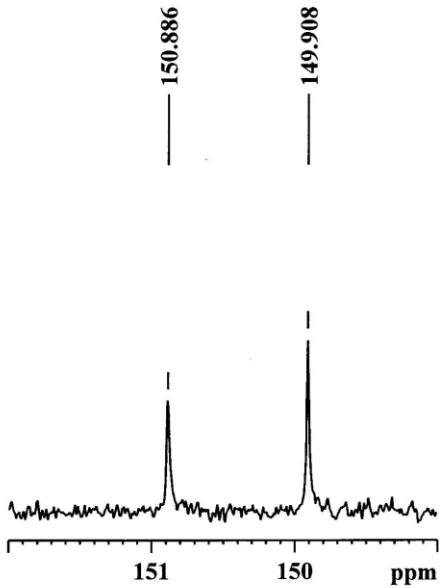
150.886
149.908
151
150
ppm

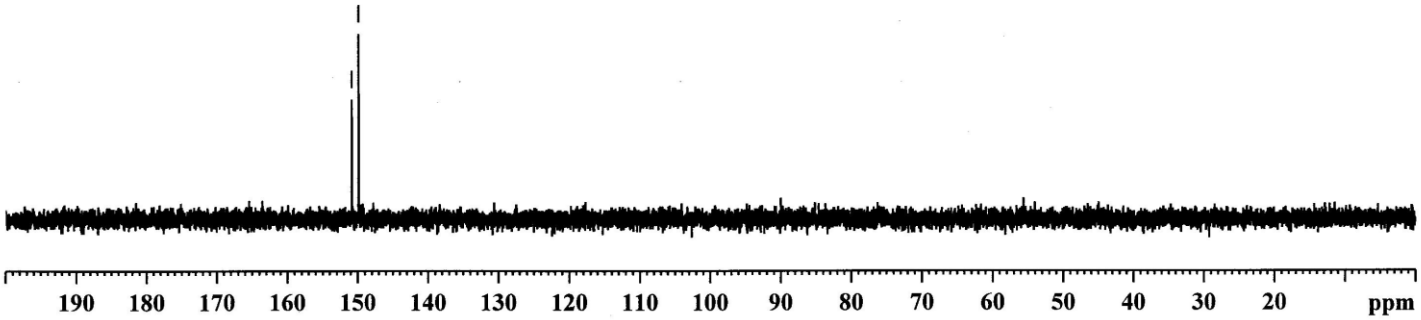
190
180
170
160
150
140
130
120
110
100
90
80
70
60
50
40
30
20
ppm